Report from the Parallel Session

S. Brodsky (SLAC)

5-2-01

- K. Zyablyuk (ITEP) — OPE analysis of τ-decays
- Y. Srivastava (North Eastern) — α_s and R via disp. rel.
- S. Pacetti (Perugia) — Space-like to Timelike Amp
- C. Vogt (Wuppertal) — $\gamma^*\gamma^* \to \pi^0, \ldots$
- S. Dubnicka (Bratislava) — Hyperon Form Factors
- C. R. Ji (North Carolina) — Time-like Exclusive
- Haiming Hu (IHEP) — Hadronization + Lund
- D. C. Peaslee (Maryland) — Vector Meson Radial Excit

All interesting, often surprising physics

K. Zyablyuk

QCD sum rule analysis of V and A current correlators from τ-decay data

based on:

B. Ioffe and KZ
hep-ph/0010089, to appear in Nucl. Phys. A

B. Geshkenbein, B. Ioffe and KZ
hep-ph/0104048

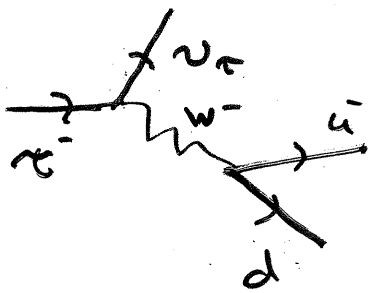

$\Rightarrow$ hadrons

Study both V, A correlators $q^2 = s$

$$i \int d^4x \, e^{iq\cdot x} \langle 0 | J_\mu(x) J_\nu^+(0) | 0 \rangle$$

$$= \left(q^\mu q^\nu - g^{\mu\nu} q^2\right) \Pi^{(1)}(q^2) + q^\mu q^\nu \Pi^{(2)}(q$$

$$V_1(q^2) = 2\pi \, \mathrm{Im}\, \Pi_V^{(1)}(q^2)$$

$$a_1(q^2) = 2\pi \, \mathrm{Im}\, \Pi_A^{(1)}(q^2)$$

measured for $0 < q^2 = s < m_\tau^2$

* $V - a$: no leading twist contrib from PQCD!

$$\Pi_V^{(1)}(s) - \Pi_A^{(1)}(s) = \sum_{k \geq 2} \frac{O_{2k}^{V-A}}{(-s)^k}$$

Borel Transform: $\otimes \frac{1}{(k-1)!}$ improves convergence

Spectral functions (EXP)

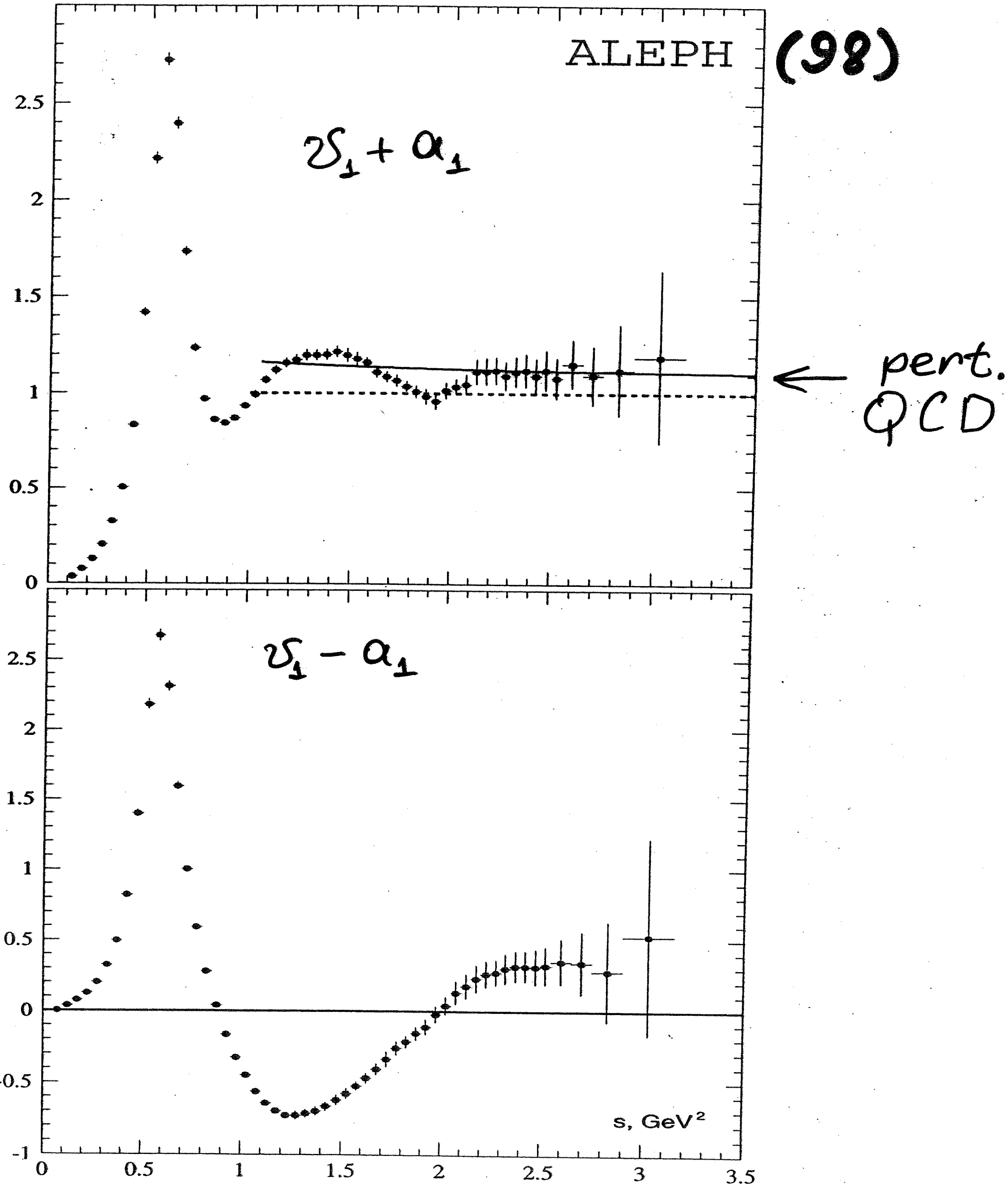

Data files taken from:

http://alephwww.cern.ch/ALPUB/paper/paper.html

QCD expressions for the correlators

$$\Pi_V^{(1)}(s) - \Pi_A^{(1)}(s) = \sum_{k\geq 2} \frac{O_{2k}^{V-A}}{(-s)^k}$$

$$\Pi_V^{(1)}(s) + \Pi_A^{(1)}(s) = -\frac{1}{2\pi^2} \ln \frac{-s}{\mu^2} + \text{higher loops} + \sum_{k\geq 2} \frac{O_{2k}^{V+A}}{(-s)^k}$$

Operator Product Expansion

Region of validity of series

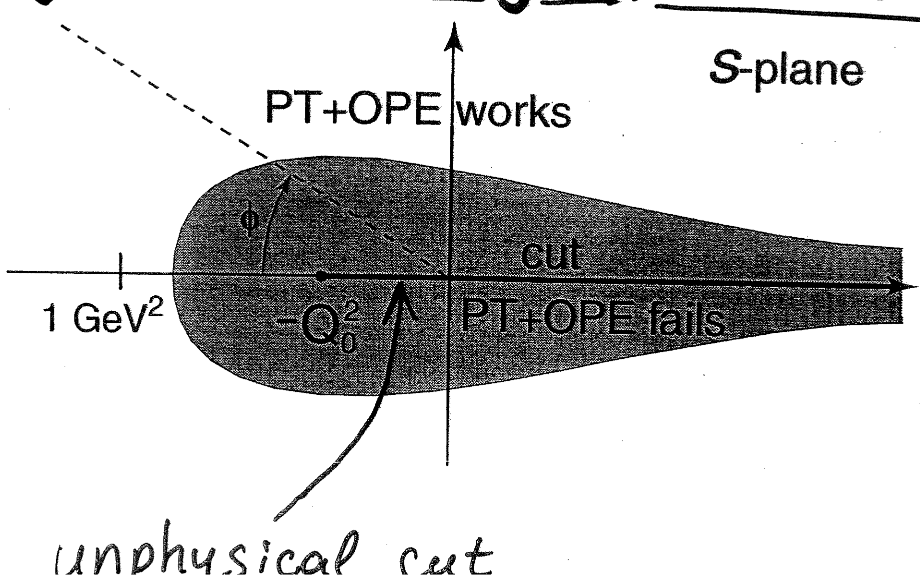

To separate the operators and f_π^2 from each other, we put Borel parameter complex $M^2 e^{i\varphi}$:

$$\int_0^\infty e^{-\frac{s}{M^2}\cos\varphi} \sin\left(\frac{s}{M^2}\sin\varphi\right)(v_1-a_1)(s)\frac{ds}{2\pi^2 M^2}$$

$$= -\sum_{k\geq 2} \frac{\sin((k-1)\varphi)}{(k-1)!}\,\frac{O_{2k}^{V-A}}{M^{2k}}$$

$\varphi = \frac{\pi}{3}$: no O_8

$\varphi = \frac{\pi}{4}$: no O_{10}

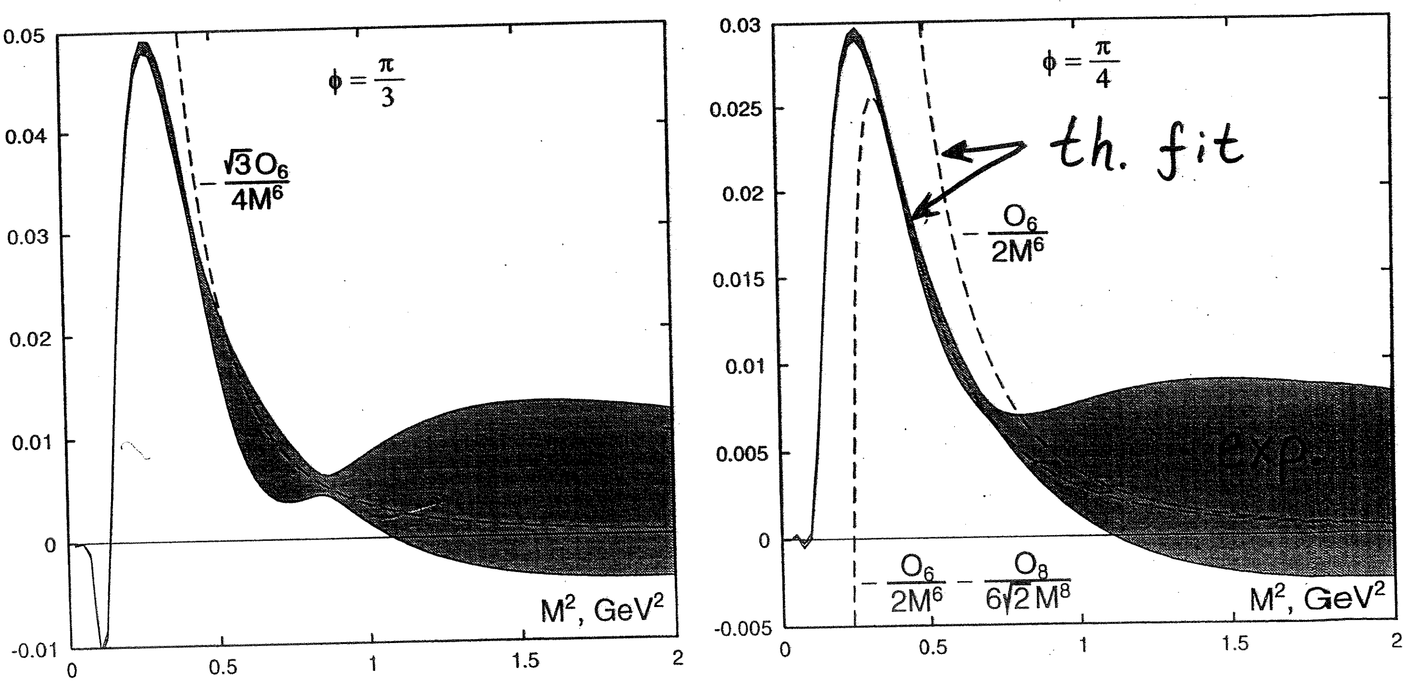

Result of fit:

$$O_6^{V-A} = -(6.8 \pm 2.1) \times 10^{-3}\ \mathrm{GeV}^6$$

$$O_8^{V-A} = (7 \pm 4) \times 10^{-3}\ \mathrm{GeV}^8$$

O_6^{V-A} is ~ 2 times larger, than what QCD and low-energy theorems predict. $\Rightarrow$

$m_u + m_d \approx 9$ MeV rather than 12 MeV at 1 GeV^2?

Factorization fails?

Very large α_s-corrections?

V+A :

Repeat analysis with $M^2 \to M^2 e^{i\phi}$

Find
$$\left\langle \frac{\alpha_s}{\pi} G^2 \right\rangle = 0.006 \pm 0.012 \text{ GeV}^4$$

$$(0.012 \text{ GeV}^4 : \text{SVZ})$$

$$\alpha_s^{\overline{MS}}(m_\tau^2) = 0.330 \qquad (\text{usually } 0.355)$$

$\therefore$ Perturbative terms dominate at $s > 1 \text{ GeV}^2$;

operator terms are small!

* PEP-N : repeat analysis for V, $I = 0, 1$

SUMMARY

⊕ V−A polarization operator is well described by OPE for $Q^2 \gtrsim 1\ \mathrm{GeV}^2$

⊖ O_6^{V-A} is ~ 2 times larger, than expected from QCD and low-energy theorems.

⊕ V+A polarization operator is well described by purely perturbative terms for $Q^2 \gtrsim 1\ \mathrm{GeV}^2$

⊖ Theoretical and experimental accuracy is not enough to specify the value of the gluonic condensate $\langle \frac{\alpha_s}{\pi} G^2 \rangle$; However it is likely to be much lower, than standard SVZ value $0.012\ \mathrm{GeV}^4$

The Inverse Problem: Extracting Time-Like from Space-Like Data

R. Baldini, S. Dubnička, P. Gauzzi, S. Pacetti,
E. Pasqualucci and Y. Srivastava

- Pion and Nucleon Form Factors (FF)

- Dispersion Relation (DR) for the modulus and integral equation

- Solving the integral equation

- Testing the Regularization method

- The Nucleon time-like FF

- Isospin Components

- Conclusions

Testing the Regularization Method$_1$

We have used the time-like Pion FF (data for $4m_\pi^2 \le s \le m_{J/\Psi}^2$ and PQCD asymptotic behaviour for $s > m_{J/\Psi}^2$) to reobtain the space-like FF according to (i) subtracted and (ii) unsubtracted DR

$$\text{(i)}: \log(G(t)) = \frac{t\sqrt{s_0 - t}}{\pi} \int_{s_0}^{\infty} \frac{\log|G(s)|}{s(s-s_0)\sqrt{s-t}} ds$$

[redacted]

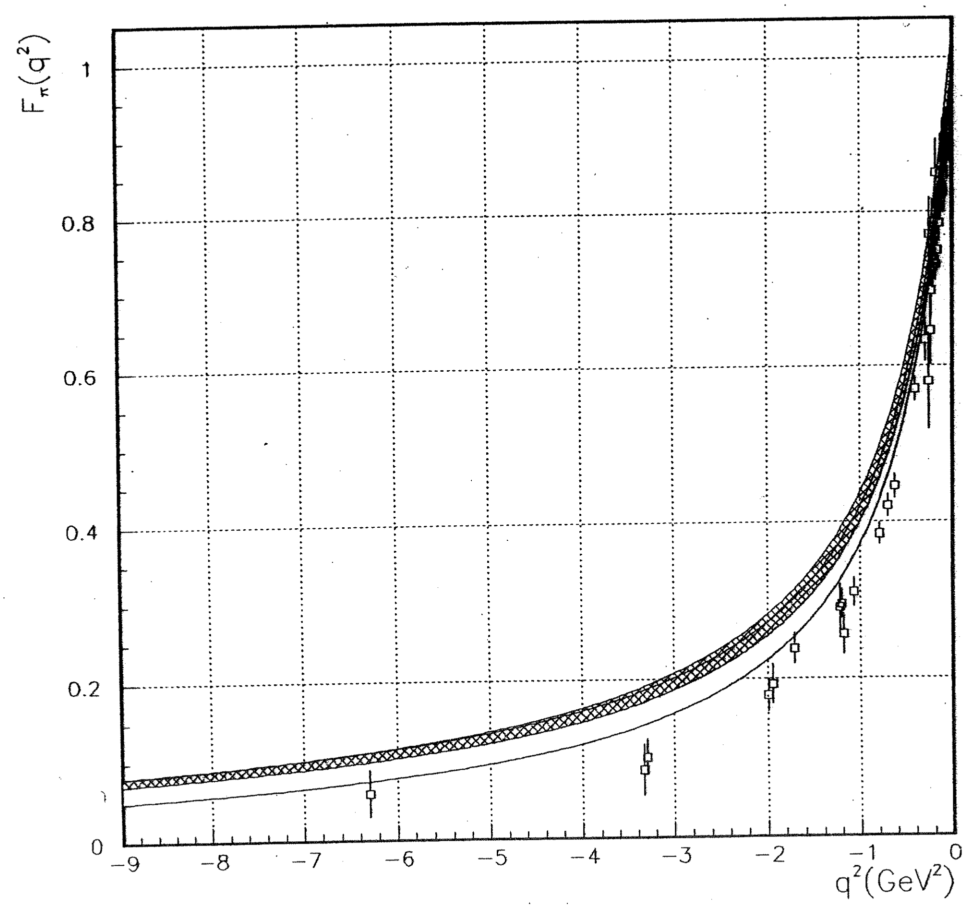

$F_\pi(s)$ $\Rightarrow$ spacelike $F_\pi(t)$

$4 m_\pi^2 < s < M_{J/\psi}^2$

data

Testing the Regularization Method$_2$

In order to fix the τ parameter, the space-like (DR) and the time-like (experimental data) Pion FF (yellow area) have been used as input in the integral equation to retrieve the time-like pion FF (gray area) in the unphysical region

$$\log(G(t)) - I(t) = \frac{t\sqrt{s_0 - t}}{\pi} \int_{s_0}^{s_2} \frac{\log|G(s)|}{s(s-t)\sqrt{s-s_0}} ds$$

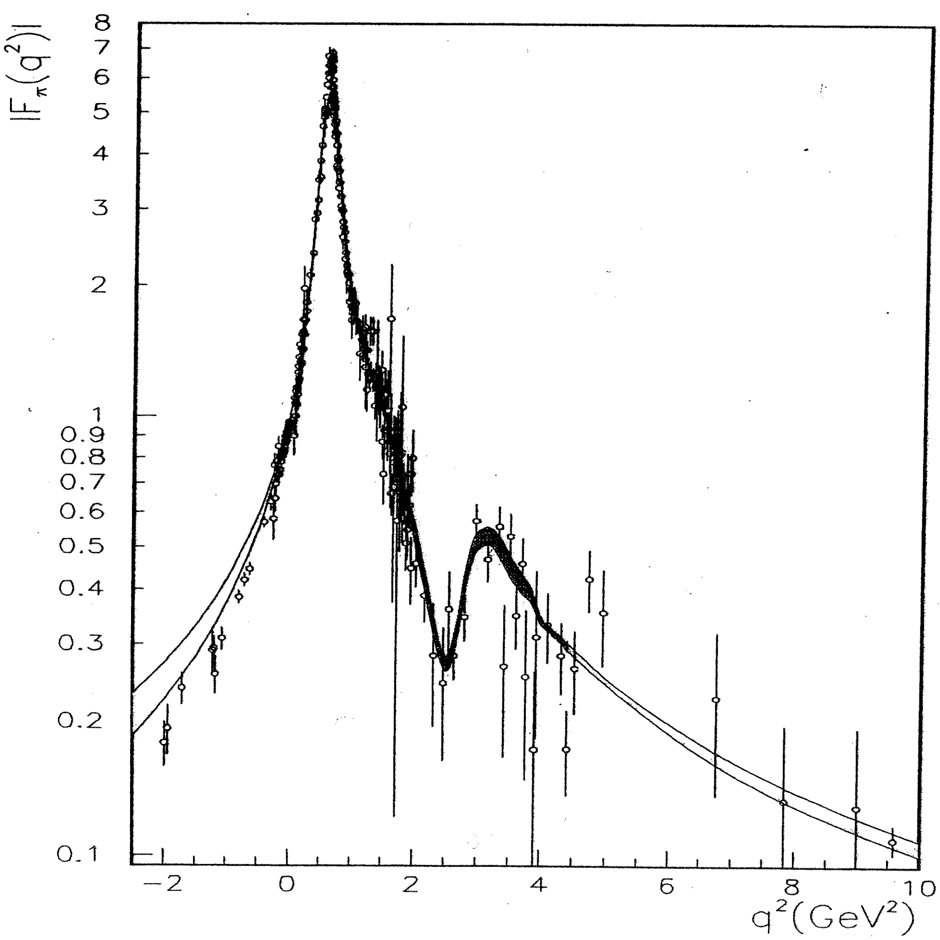

$\tau \sim m_\pi$ ← "dumping" param in num. analysis"

$F_\pi(q^2)$ small

$\Longrightarrow$ $F_\pi(q^2)$

The Nucleon time-like Magnetic FF

To extract the Nucleon FF near threshold, where the data show a steep variation, in the interval $[s_1 - \Delta, s_1 + \Delta]$ we use the DR:

$$\frac{t}{\pi}\int_{s_1-\Delta}^{s_1} \frac{\log|G_1(s)|}{s(s-t)\sqrt{s-s_0}}ds + \frac{t}{\pi}\int_{s_1}^{s_1+\Delta} \frac{\log|G_1(s)|}{s(s-t)\sqrt{s-s_0}}ds +$$

with: $G_M = G_0 G_1$ in this interval, $G_M = G_0$ outside.

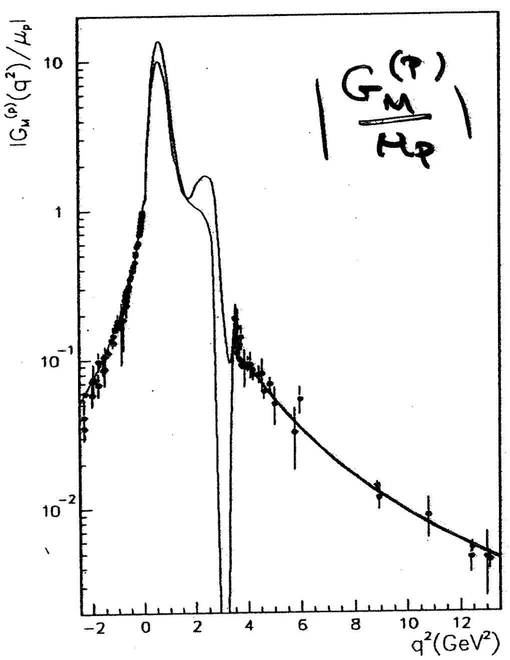

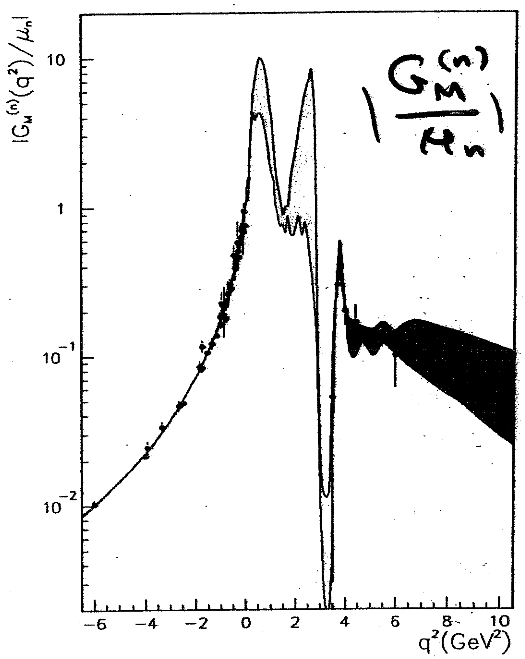

[redacted] [redacted]

[redacted] [redacted]

Isospin Components of the Nucleon Magnetic FF

The isospin components of the magnetic FF are:

$$G_M^S = \frac{1}{2}(G_M^p + G_M^n) \qquad G_M^V = \frac{1}{2}(G_M^p - G_M^n)$$

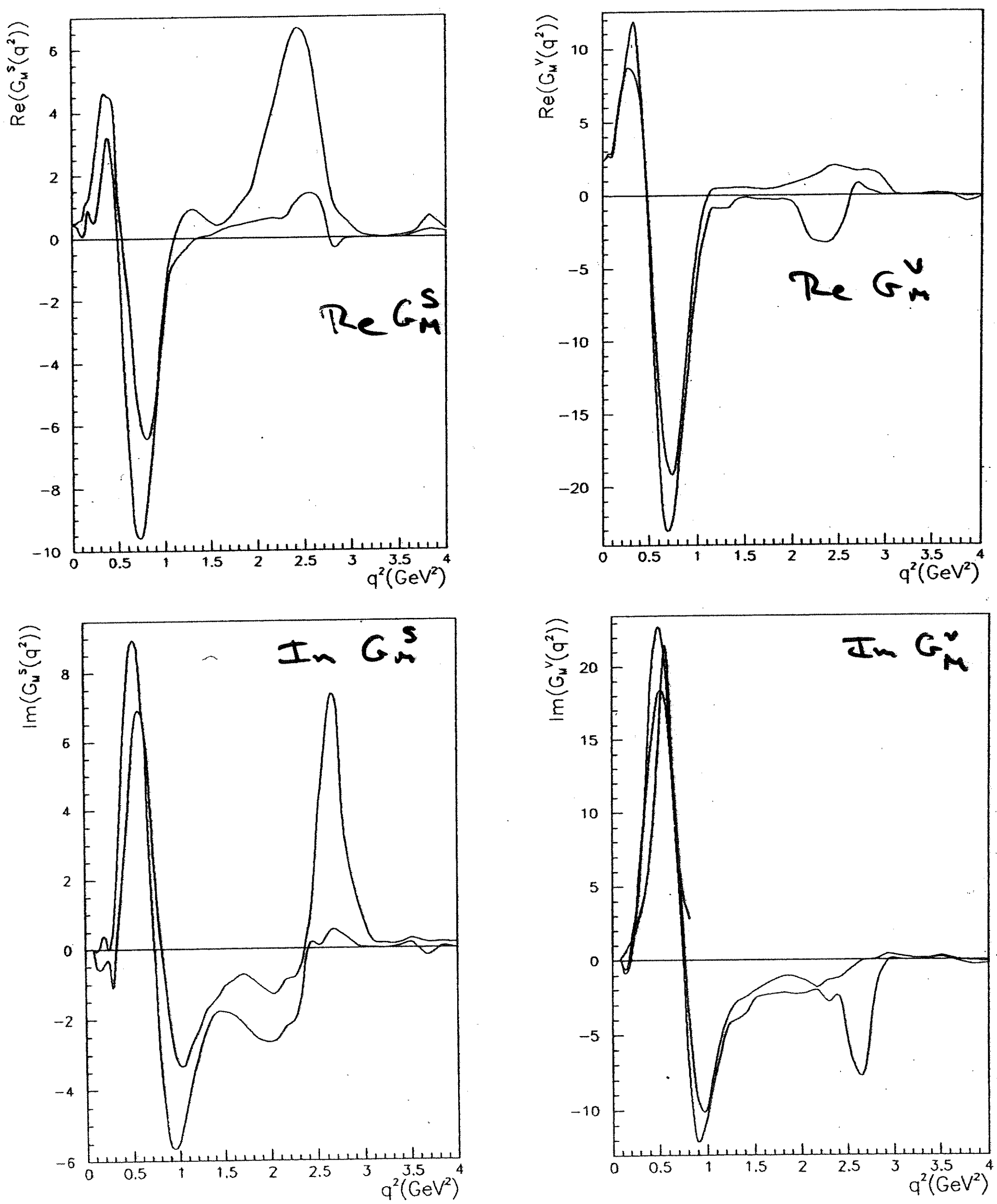

0 $\quad q^2 \quad$ 4 GeV^2

Conclusions

- The Nucleon time-like magnetic FF in the unphysical region has been obtained in a model independent way by means of a DR for $\log|G|$.
- Resonances have been found consistent with $\rho(770)$ and $\rho'(1600)$ masses, however very large widths are obtained
- No sizeable Φ contribution has been found
- Phases for the Nucleons are consistent with the expectations: $\delta_N \to 360^o$
- There is an interference pattern near Nucleon threshold ($M \sim 1.88\, GeV$)
- Various super-convergence sum rules are obeyed by Nucleon FF. Our analysis indicates that $\mathrm{Im}F_\pi$ does not change sign, this would suggest that (neglecting logarithmic factors):

$$|F_\pi(s)| \to |s|^{-1+\epsilon} \text{ as } |s| \to \infty \qquad (\epsilon > 0)$$

Three applications of the dispersive techniq

Yogendra Srivastava
(Perugia & Northeastern)

1. $\boxed{R_{had}(s)}$: Crystal Ball vs. MARK I
   $\sqrt{s} = (5 \div 7.5)$ GeV
   (Pacetti & Y.S.)

2. $\boxed{\alpha_s(s)}$: Low and Medium s
   τ decay
   (Pancheri / Pacetti & Y.S.)

3. $\boxed{\text{Confinement}}$: "Wrong" sign of $\mathrm{Im}\,\alpha(s)$
   ↳ instability of the perturbative vacuum

   (Widom & Y.S.)

Crystal Ball & Mark I

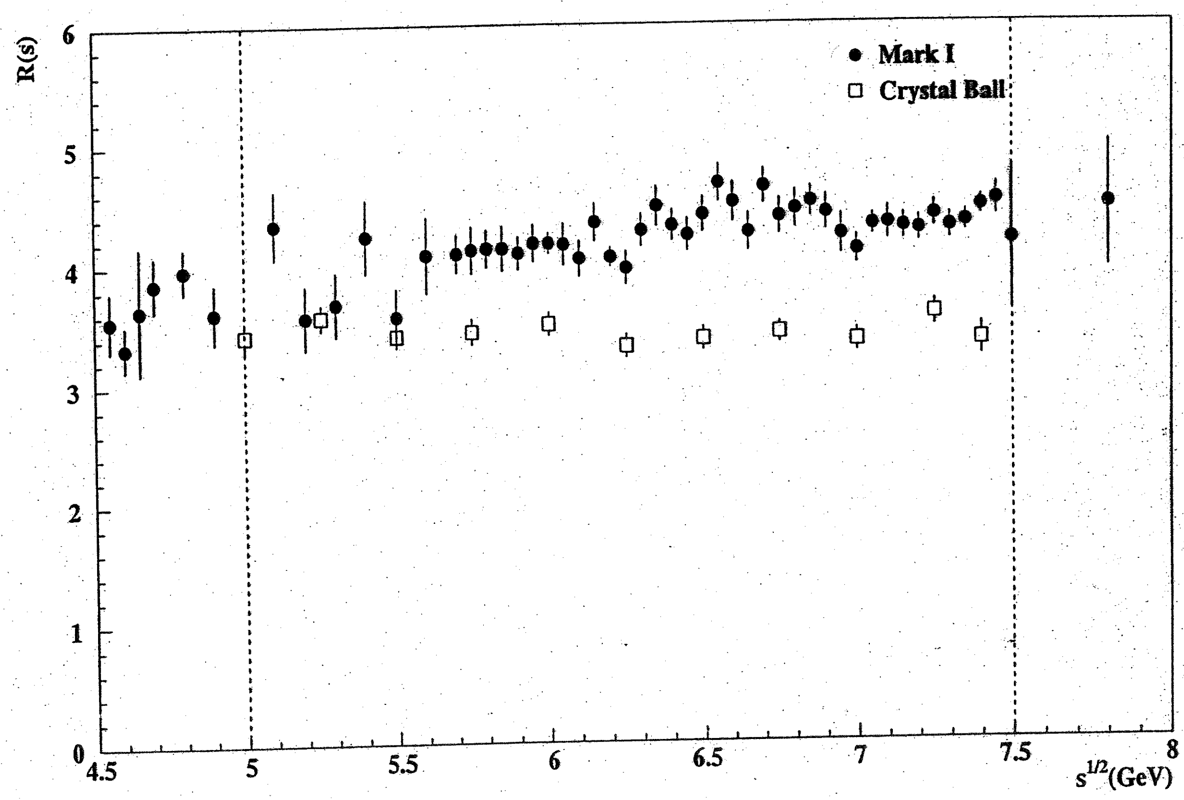

Solution with the u, d, s, c, b quarks

$\mathcal{R}(s)$

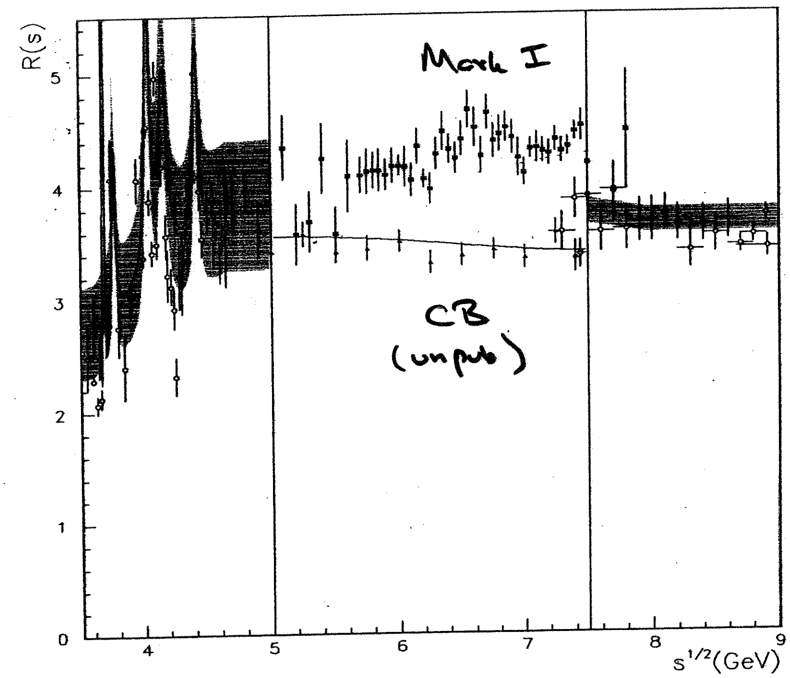

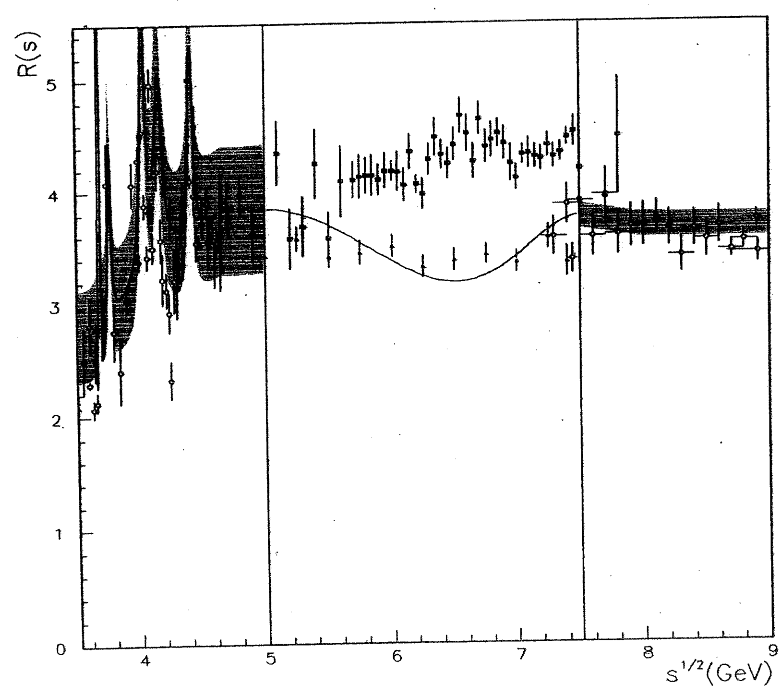

Solution with the $u, d, s, c, b + Y$ quarks

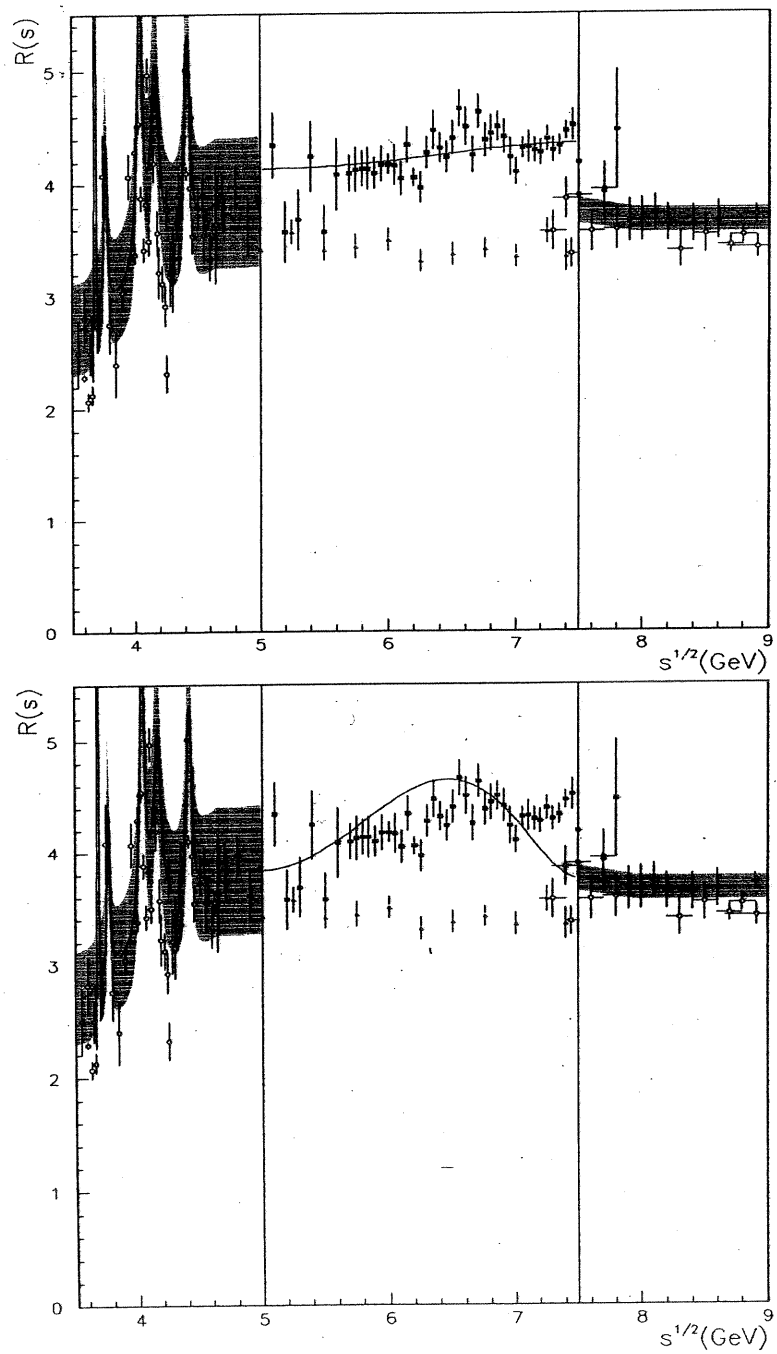

Y: spin 0 quark

$e_Y = 1/3$

- Perturbative $\alpha(s)$ has the wrong analyticity. E.g. 1-loop AF formula

$$\alpha_{1\text{-loop}}(s) = \frac{1}{b} \frac{1}{\ln(-s/\Lambda^2)}$$

has a pole at space-like $\boxed{-s = \Lambda^2}$

- Higher loops suffer from the same disease
- Analyticity based on unitarity forbids any singularity for space-like $s < 0$
- Cures: **Analytic Perturbation Theory**

1. **Bogoliubov, Shirkov....**

- **Compute the imaginary part from AF**

$$\mathrm{Im}\,\alpha_1(s) = \frac{1}{b} \frac{\pi}{(\ln s/\Lambda^2)^2 + \pi^2} \vartheta(s)$$

then use dispersion relation to compute the Real part. Thanks to $\sim \frac{1}{(\ln s/\Lambda^2)^2}$ unsubtracted dispersion relation converges.

$$\alpha_I(s) = \frac{1}{b}\left[\frac{1}{\ln(-s/\Lambda^2)} + \frac{\Lambda^2}{\Lambda^2 + s}\right]$$

The second term cancels the unwanted

Analytic Models for α_{QCD}

$$\alpha(Q^2) = \frac{1}{b}\left[\frac{1}{\log(Q^2/\Lambda^2)} + \frac{\Lambda^2}{\Lambda^2 - Q^2}\right]$$

I.L.Solovtsov, D.V.Shirkov *Theor.Math.Phys.* **120** (1999) 1220, *Teor.Mat.Fiz.* **120** (1999) 482; hep-ph/9909305

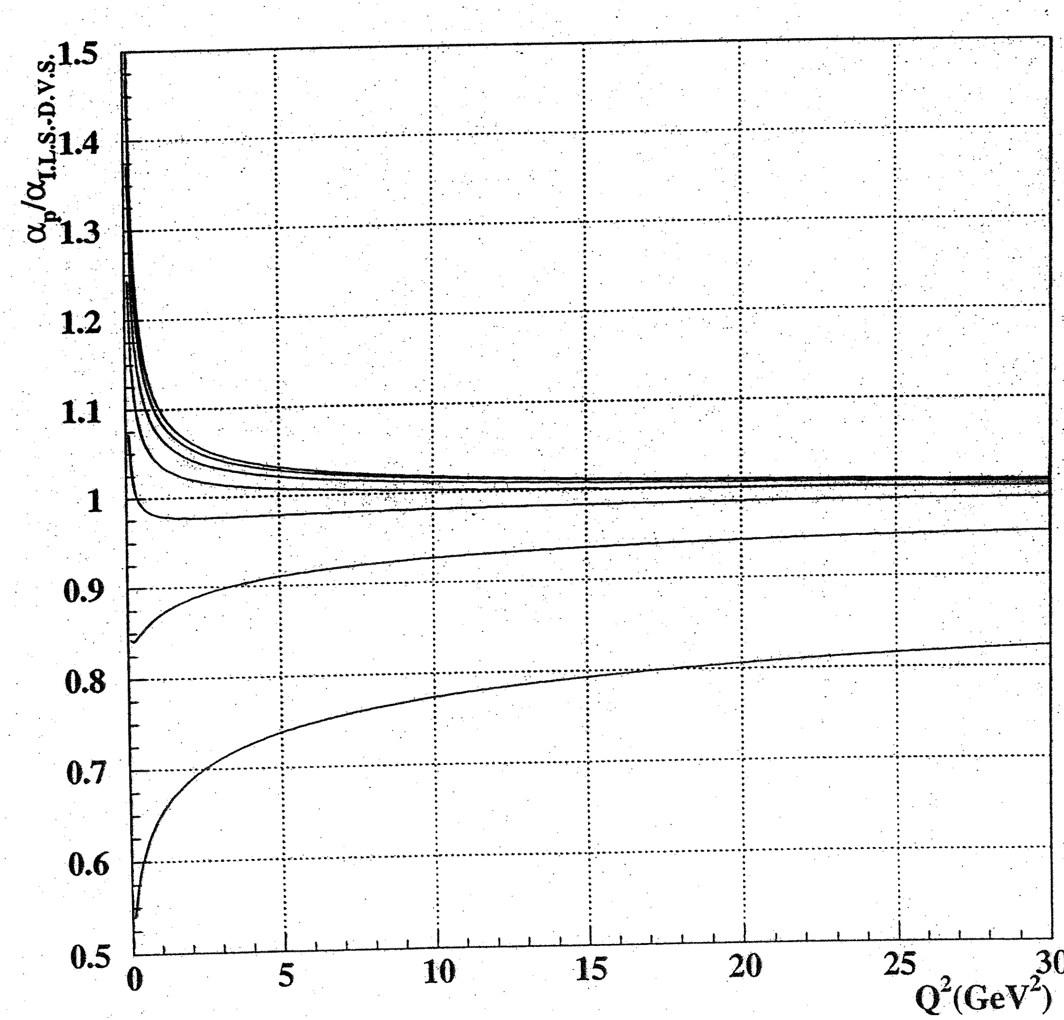

Srivastava:

$$\epsilon(s) = \frac{1}{\alpha(s)}$$

e.g. in QED

$$\frac{\alpha_0}{r} \Rightarrow \frac{\alpha_0}{\epsilon r}$$ in materials
ϵ = dielectric constant

Asymptotic freedom

$$\epsilon(s) = b \ln(-s/\Lambda^2) \quad \text{L.O}$$

$$\text{Im } \epsilon(s) = -\pi b \, \Theta(s) \quad \text{L.O.}$$

* negative Im $\epsilon(s)$ $\Rightarrow$ like an "amplifier"
$\Rightarrow$ unstable vacuum

Generalization

$$\text{Im } \epsilon(s) = -\pi b \left(\frac{s}{s+\Lambda^2}\right)^p \quad 0<p<1$$

Fit to τ decay

$\Lambda \sim 300$ MeV, $p \sim 0.5$ to 0.8

- An artificially pumped system such as a MASER or a spin system has

$$T_N < 0$$

$$\rightarrow \quad \mathrm{Im}\, \epsilon(s) < 0$$

and the system is unstable.

- We have shown that such a system exhibits a Klein paradox for photons.

- Perturbative QCD ground state has $\mathrm{Im}\, \epsilon(s) < 0$ and thus is expected to be unstable

$$\left.\begin{matrix} \text{quarks} \\ + \\ \text{glue} \end{matrix}\right\} \xrightarrow[\text{as}]{\text{manifest}} \underline{\text{hadrons}}.$$

α_p space-like

$$\mathrm{Im}(\epsilon(q^2)) = -b\pi\theta(q^2)\frac{1}{1+\left(\frac{\Lambda^2}{q^2}\right)^p} \qquad p > 0$$

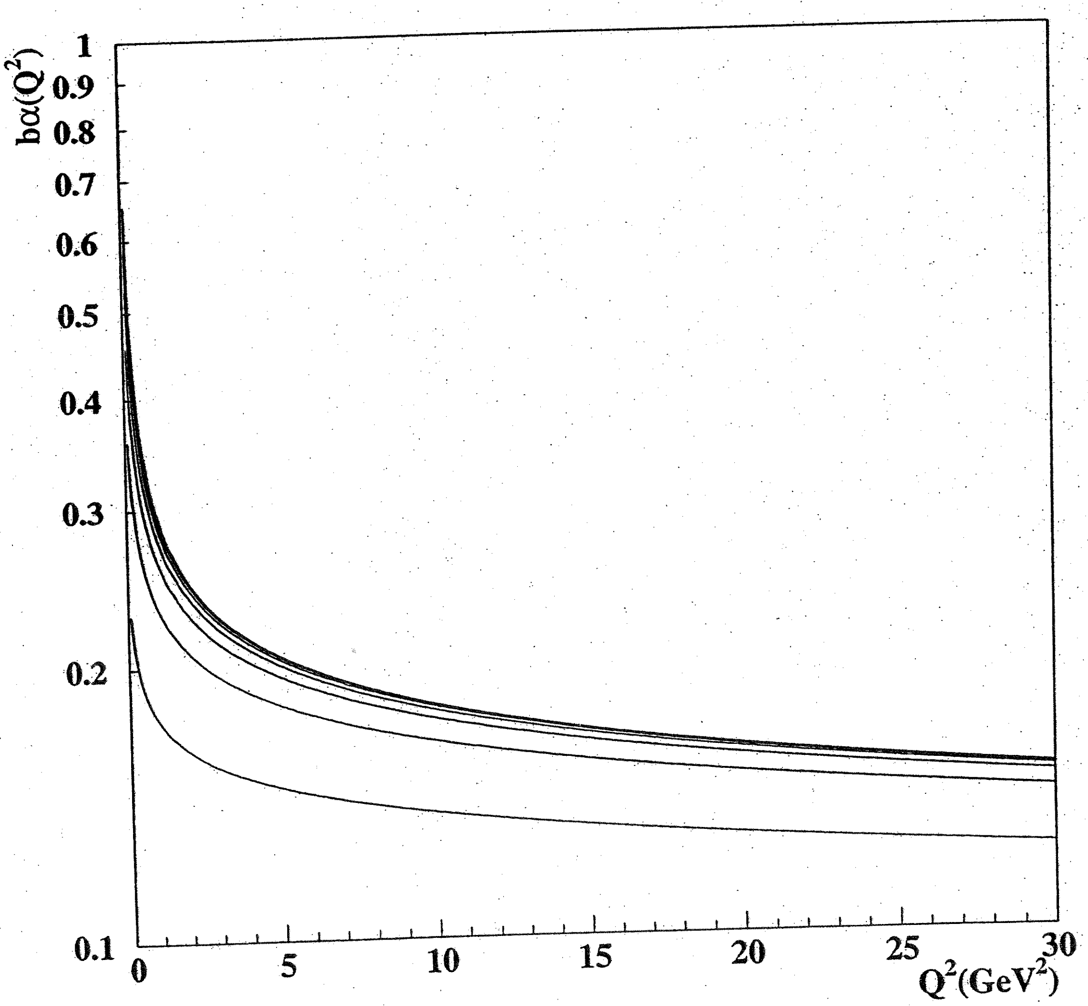

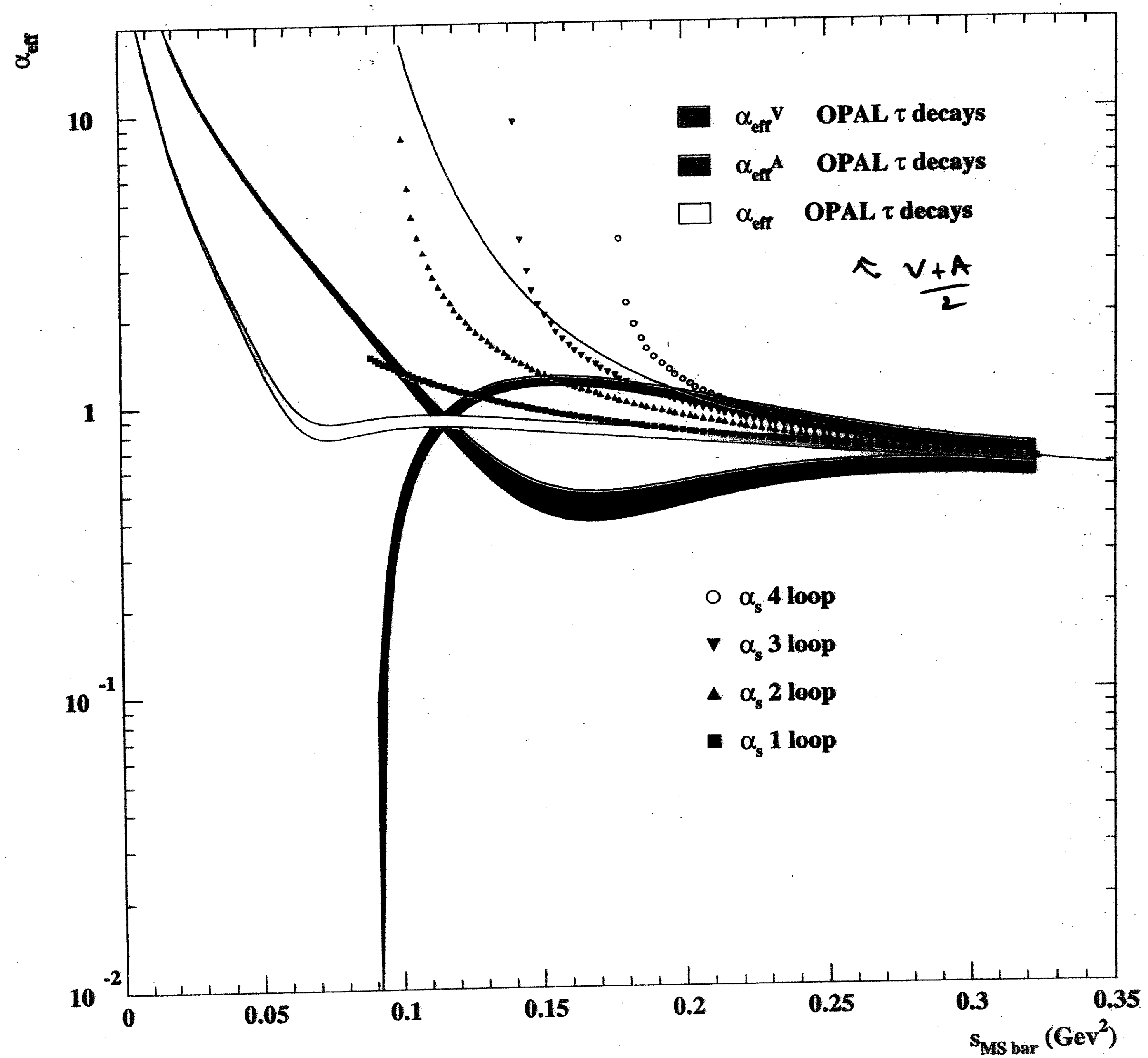

α_{eff}
10
1
10^{-1}
10^{-2}
0
0.05
0.1
0.15
0.2
0.25
0.3
0.35
$s_{MS\ bar}$ (Gev^2)
α_{eff}^V OPAL τ decays
α_{eff}^A OPAL τ decays
α_{eff} OPAL τ decays
$\frac{V+A}{2}$
α_s 4 loop
α_s 3 loop
α_s 2 loop
α_s 1 loop

Menke

C. R. Ji : Timelike Processes

For spacelike form factors $\langle P+q | J^{\mu}(0) | P \rangle$

choose $q^+ = 0$, $q^2 = q^+ q^- - q_\perp^2 = -q_\perp^2$

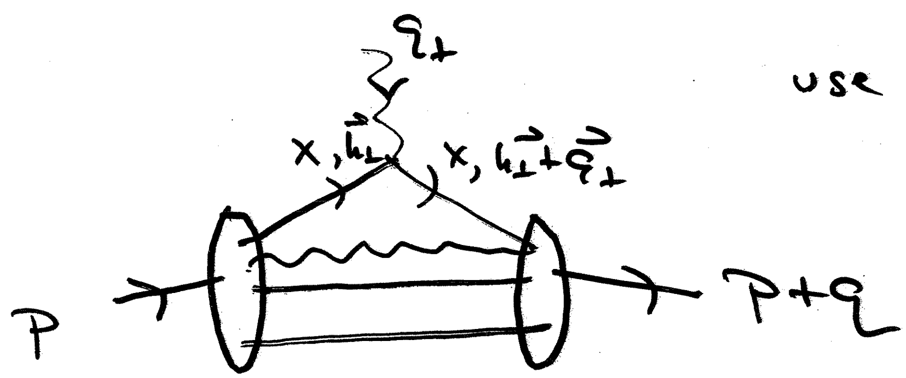

use J^+ current

$$F_{\lambda\lambda'}(q^2) = \sum_{n \geq 3} \int \psi_n(x, \vec{k}_\perp)\, \psi_n^{\dagger}(x, \vec{k}_\perp + (1-x)\vec{q}_\perp, \dots)$$

diagonal overlap !

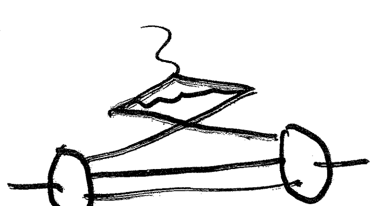

no Z-graphs, zero modes, ..

no vacuum graphs

Exact formula in light-front QCD

Drell Yan West
SJB + Drell

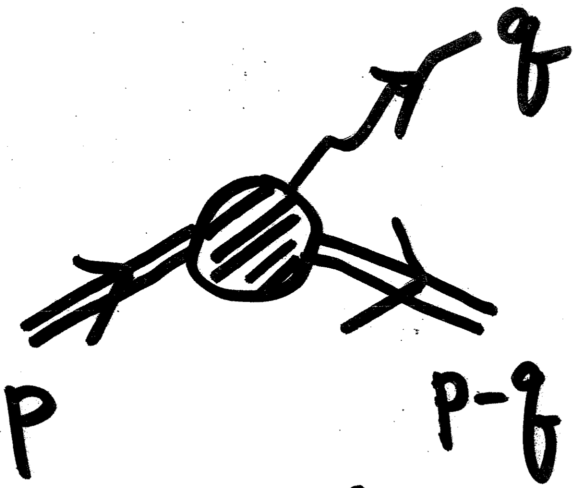

$\boxed{q^2 > 0}$

$=$

$\sum_n$

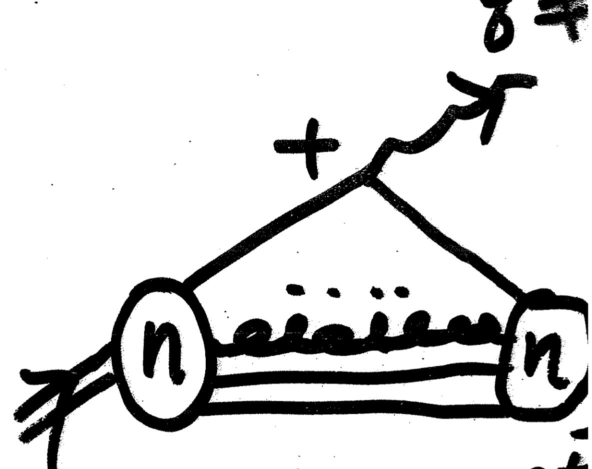

$q^2 = q^+ q^- - \vec{q}_\perp^{\,2}$

$+ \sum_n$

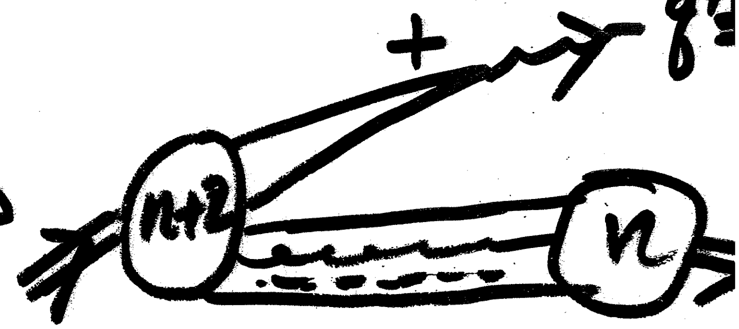

Brodsky & Hwang, NP B543, 239 ('98

$\approx$

CQM

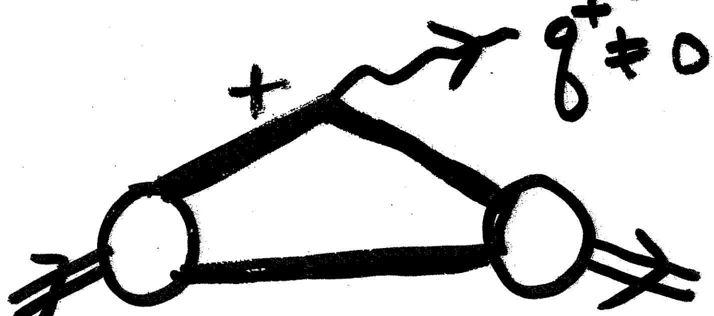

$+$

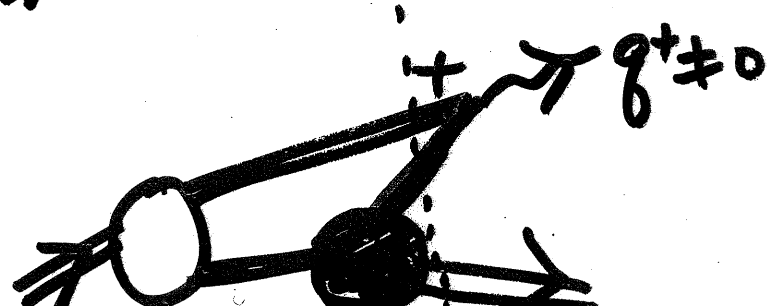

Non-wavefunction-vertex
or Embedded State

Bakker & Ji, PRD 62, 074014 ('00)

Choi & Ji, Nucl. Phys. A679, 735 (2001).

Analytic continuation from space-like region to time-like region.

$M_\pi = 140$ MeV

$m = 250$ MeV

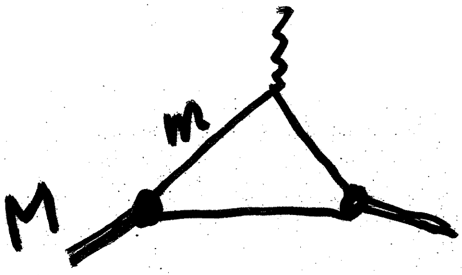

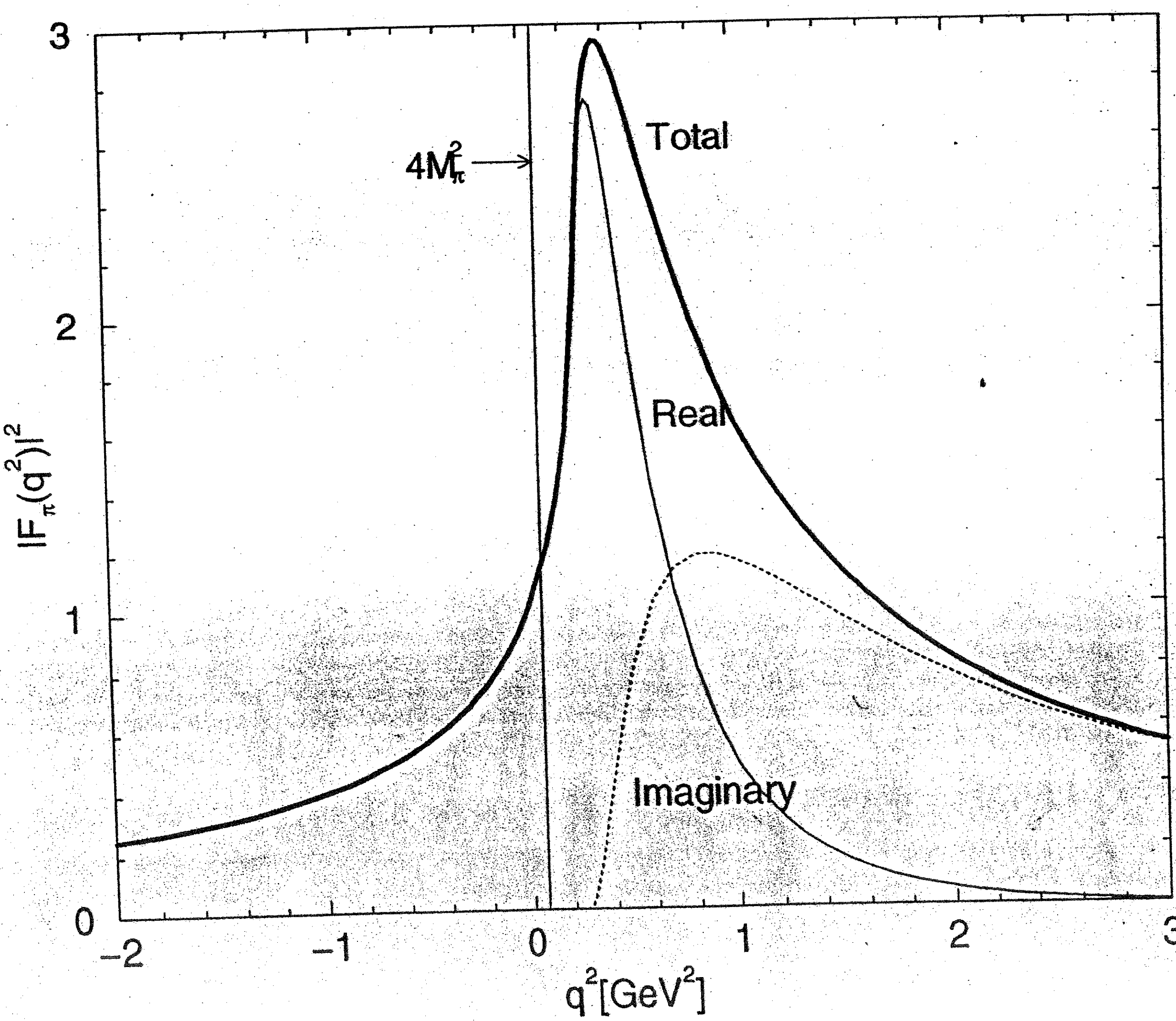

Application to Semileptonic Decay Processes

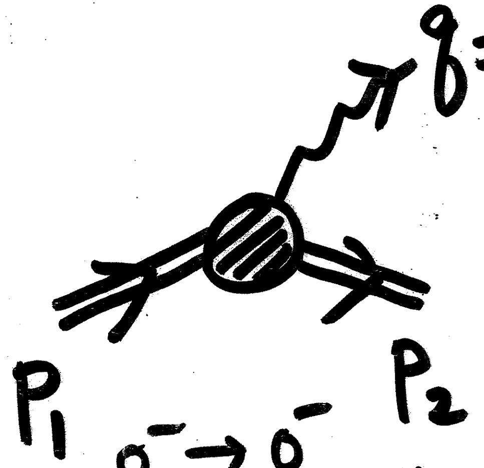

$\approx$

CQM

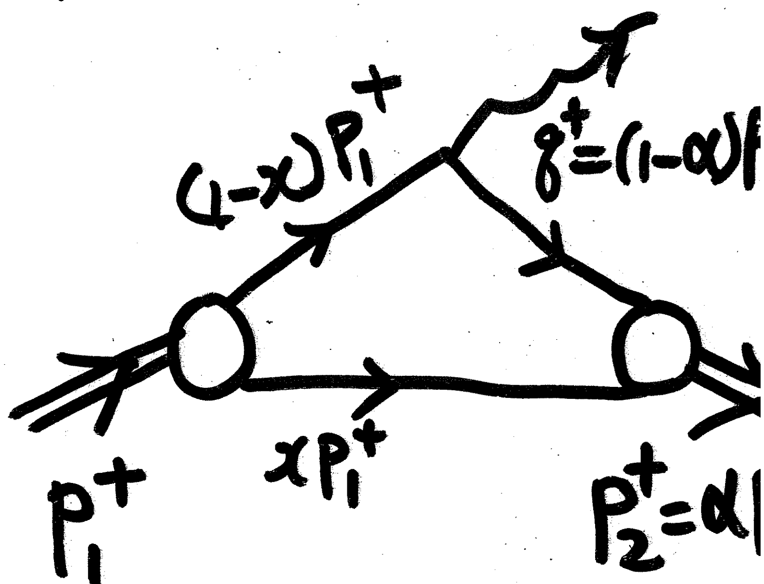

$$J^\mu = f_+(q^2)(P_1+P_2)^\mu + f_-(q^2)\, q^\mu$$

$0 < x < \alpha$

$+$

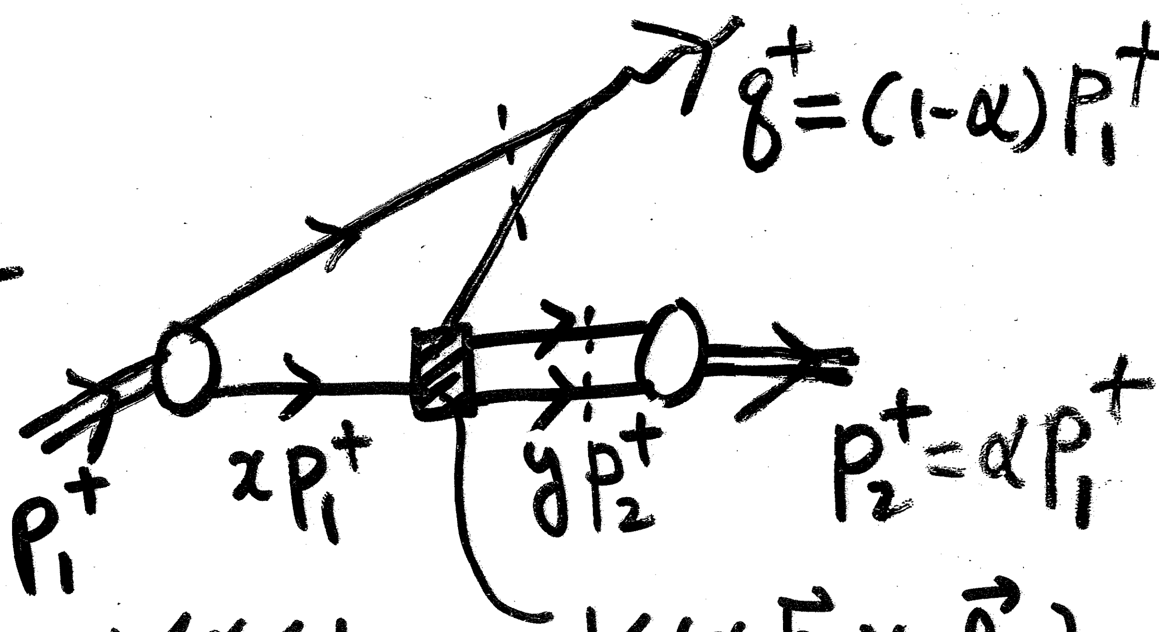

$\alpha < x < 1$

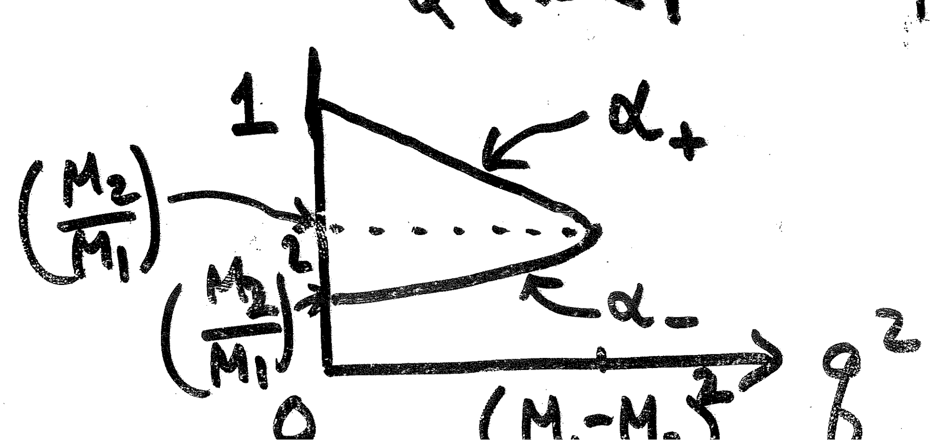

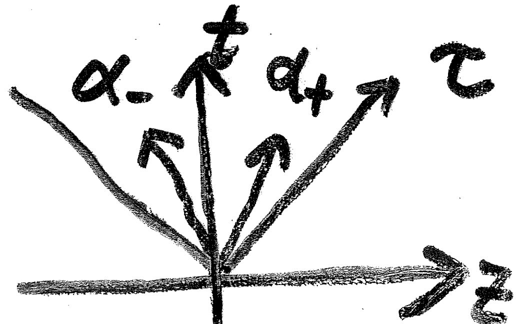

Choi & Ji, PLB460, 461 (99)
PRD59, 074015 (99)

TABLES

TABLE I. Optimized quark masses m_q[GeV] and the gaussian parameters β[GeV] for both harmonic oscillator and linear potentials obtained from the variational principle. We also include the results from the smearing function(s.f.) given in Eq.(2.12) instead of the Breit-Fermi contact term. q=u and d.

Potential	m_q	m_s	m_c	m_b	$\beta_{q\bar{q}}$	$\beta_{s\bar{s}}$	$\beta_{q\bar{s}}$	$\beta_{q\bar{c}}$	$\beta_{s\bar{c}}$	$\beta_{c\bar{c}}$	$\beta_{q\bar{b}}$	$\beta_{s\bar{b}}$	$\beta_{b\bar{b}}$
H.O.	0.25	0.48	1.8	5.2	0.3194	0.3681	0.3419	0.4216	0.4686	0.6998	0.4960	0.5740	1.8025
s.f.	0.25	0.48	1.8	5.2	0.3194	0.3703	0.3428	0.4280	0.4782	0.7278	0.5122	0.5980	1.9101
Linear	0.22	0.45	1.8	5.2	0.3659	0.4128	0.3886	0.4679	0.5016	0.6509	0.5266	0.5712	1.1452
s.f.	0.22	0.45	1.8	5.2	0.3659	0.4132	0.3887	0.4697	0.5042	0.6548	0.5307	0.5767	1.1806

TABLE II. Fit of the ground state meson masses with the parameters given in Table I. Underline masses are input data. The masses of $(\omega-\phi)$ and $(\eta-\eta')$ were used to determine the mixing angles of $\omega-\phi$ and $\eta-\eta'$, respectively.

$^1S_0$	Experiment[MeV]	H.O.[s.f.]	Linear[s.f.]	$^3S_1$	Experiment	H.O.[s.f.]	Linear[s.f.]
π	135±0.00035	135[135]	135[135]	ρ	770± 0.8	770[770]	770[770]
K	494± 0.016	470[469]	478[478]	K^*	892± 0.24	875[875]	850[850]
η	547± 0.19	547[547]	547[547]	ω	782± 0.12	782[782]	782[782]
η'	958±0.14	958[958]	958[958]	ϕ	1020±0.008	1020[1020]	1020[1020]
D	1869±0.5	1821[1821]	1836[1840]	D^*	2010± 0.5	2024[2026]	1998[1997]
D_s	1969±0.6	2005[2004]	2011[2014]	D_s^*	2112±0.7	2150[2150]	2109[2108]
η_c	2980± 2.1	3128[3123]	3171[3173]	J/ψ	3097±0.04	3257[3244]	3225[3221]
B	5279± 1.8	5235[5231]	5235[5237]	B^*	5325± 1.8	5349[5349]	5315[5314]
B_s	5369±2.0	5378[5372]	5375[5376]	$(b\bar{s})$	–	5471[5466]	5424[5423]
$(b\bar{b})$	–	9295[9353]	9657[9651]	Υ	9460± 0.21	9558[9459]	9691[9675]

$\delta(\omega-\phi)$ $\pm 4.2^\circ$ $\pm 7.8^\circ$
$\theta_{SU(3)}(\eta-\eta')$ -19.3° -19.6°

Table 4: Decay constants and charge radii for various light pseudoscalar and vector mesons. We use the $\omega-\phi$ mixing angle, $\delta_V = \theta_{SU(3)} - 35.26° = \mp 3.3°$, for the calculation of f_ρ and f_ω.

Observables	HO	Linear	Experiment
f_π [MeV]	131	130	131
f_K [MeV]	155	161	160
f_ρ [MeV]	215	246	216
f_{K^*} [MeV]	223	256	(244)
f_ω [MeV]	65 (78)	74 (89)	65
f_ϕ [MeV]	117 (108)	133 (124)	112
r^2_π [fm^2]	0.449	0.425	0.432 ± 0.016
$r^2_{K^+}$ [fm^2]	0.384	0.354	0.34 ± 0.05
$r^2_{K^0}$ [fm^2]	-0.091	-0.082	-0.054 ± 0.101

Choi & Ji
PRD59, 074015 (99)

Table 5: Decay constants[MeV] and charge radii[fm^2] for various heavy pseudoscalar and vector mesons.

References	f_D	f_{D^*}	f_{D_s}	f_B	f_{B^*}	f_{B_s}
HO	179.7	211.6	218.6	160.9	173.0	207.0
Linear	196.9	238.9	233.1	171.4	185.8	203.9
Lat.[1]	200 ± 30	–	220 ± 30	170 ± 35	–	195 ± 35
Lat.[2]	195 ± 11	–	213 ± 9	159 ± 11	–	175 ± 10
SD [3]	214	290	234	182	200	194
Expt.	< 219		$137 - 304$			
References	$r^2_{D^+}$	$r^2_{D^0}$	$r^2_{D_s^+}$	$r^2_{B^+}$	$r^2_{B^0}$	$r^2_{B_s^0}$
HO	0.182	-0.309	0.106	0.420	-0.208	-0.081
Linear	0.176	-0.301	0.101	0.438	-0.217	-0.083

[1] J. M. Flynn and C. T. Sachrajda, hep-lat/9710057. [2] MILC Collaboration, C. Bernard et al., PRL 81, 4812(1998). [3] M. A. Ivanov, Yu. L. Kalinovsky, and C. D. Roberts, PRD 60, 034018 (1999).

Choi & Ji
PLB 460, 461 (99)

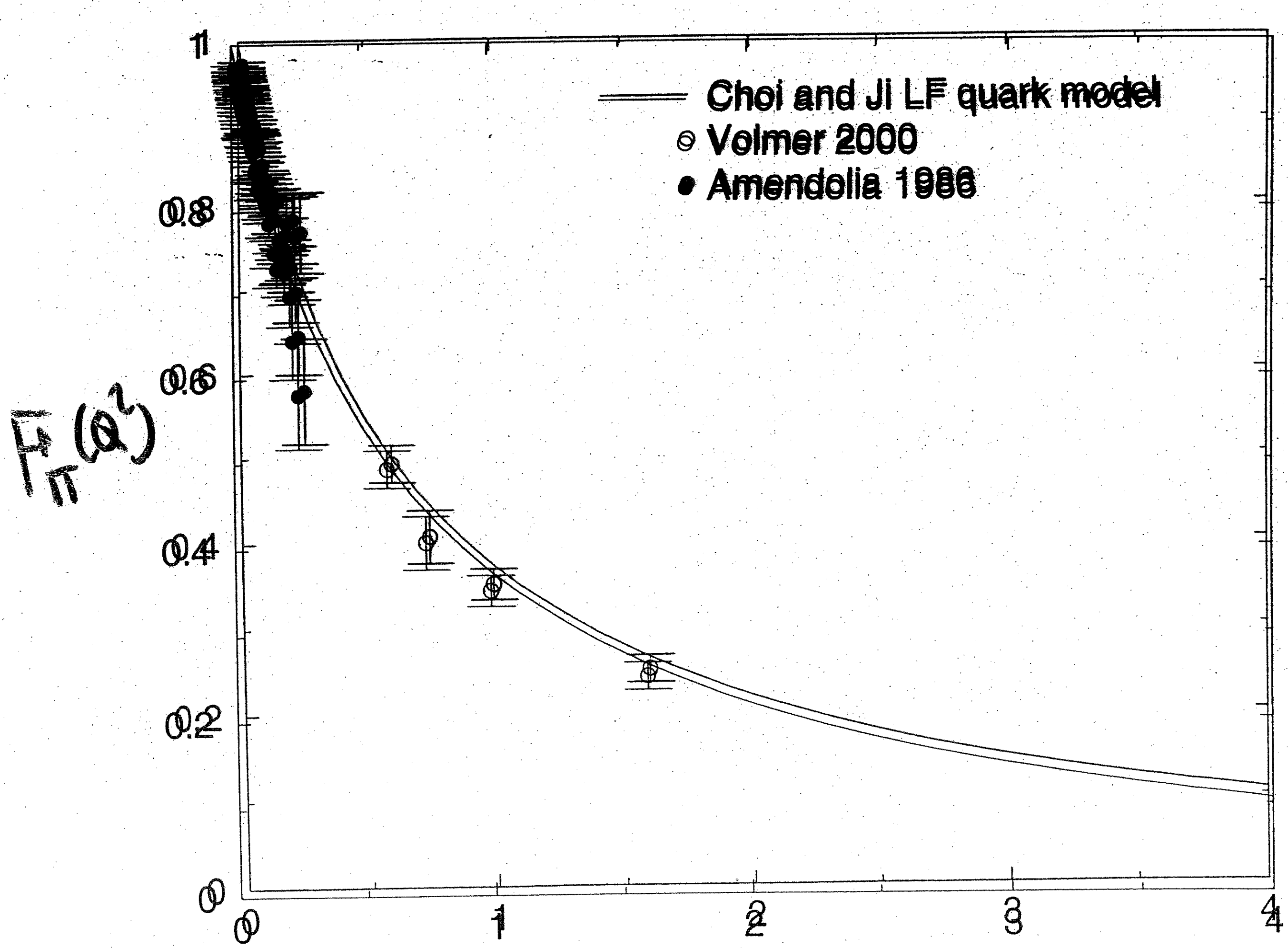

Choi and Ji LF quark model
Volmer 2000
Amendolia 1986
$F_\pi(Q^2)$
1
0.8
0.6
0.4
0.2
0
0
1
2
3
4

$G_{K\pi} = 3.95$

$$f_i(q^2) = f_i(q^2 = m_\ell^2)(1 + \lambda_i q^2/M_\pi^2) \quad (i = +, 0)$$

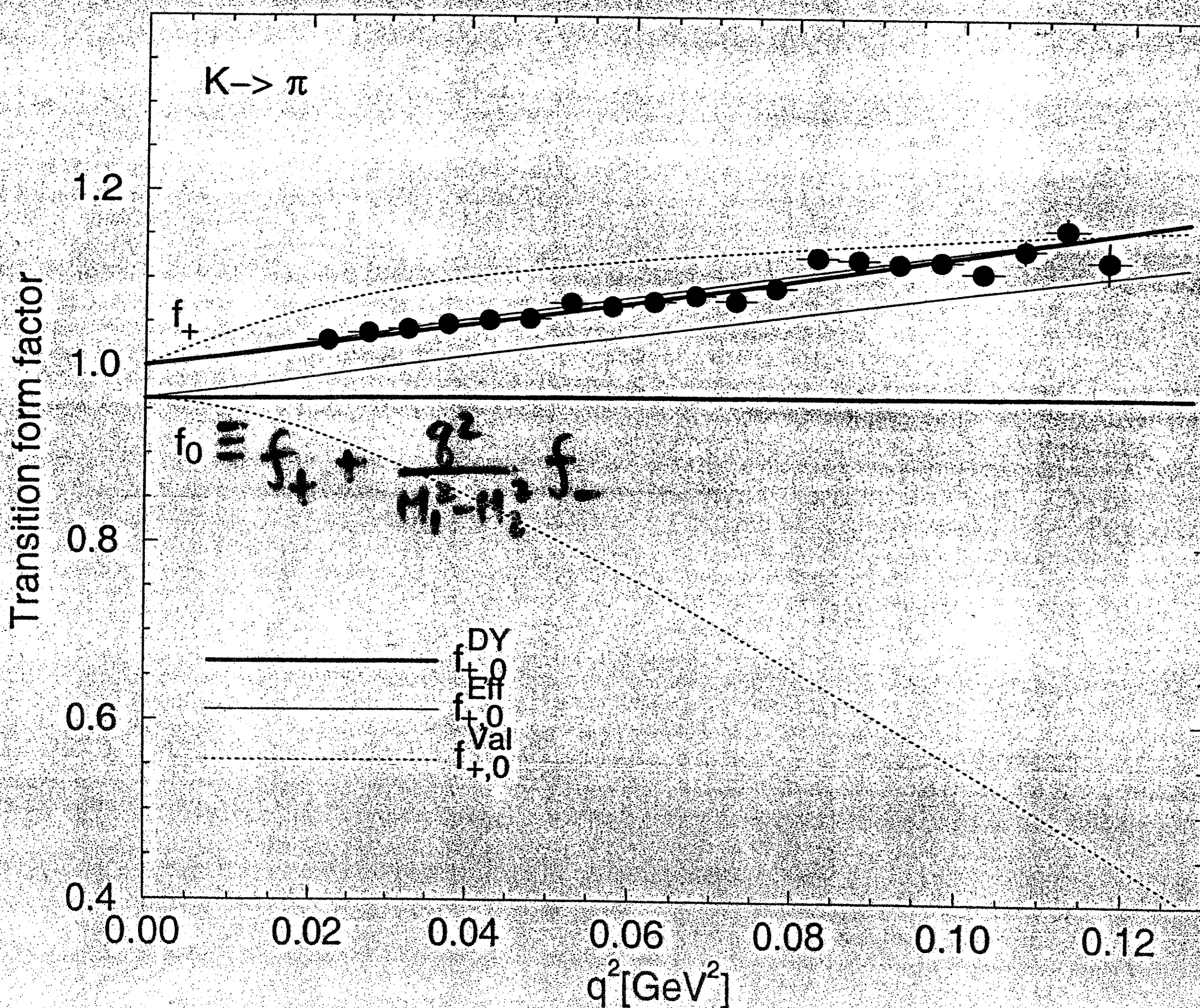

$G_{DK} = 3.5$

$f_{+(0)}(q^2) = f_{+(0)}(0) / (1 - q^2/M_{1^-(0^+)}^2)$, $M_{1^-} = 2.16\,GeV$ $(M_{D_s^*} = 2.1\,GeV)$ $M_{0^+} = 2.79\,GeV$

$|V_{cs}| = 1.04 \pm 0.16$

$Br(D^0_{e3}) = 3.73 \pm 1.24$ Expt: 3.64 ± 0.18

$Br(D^0_{\mu 3}) = 3.60 \pm 1.19$ 3.22 ± 0.17

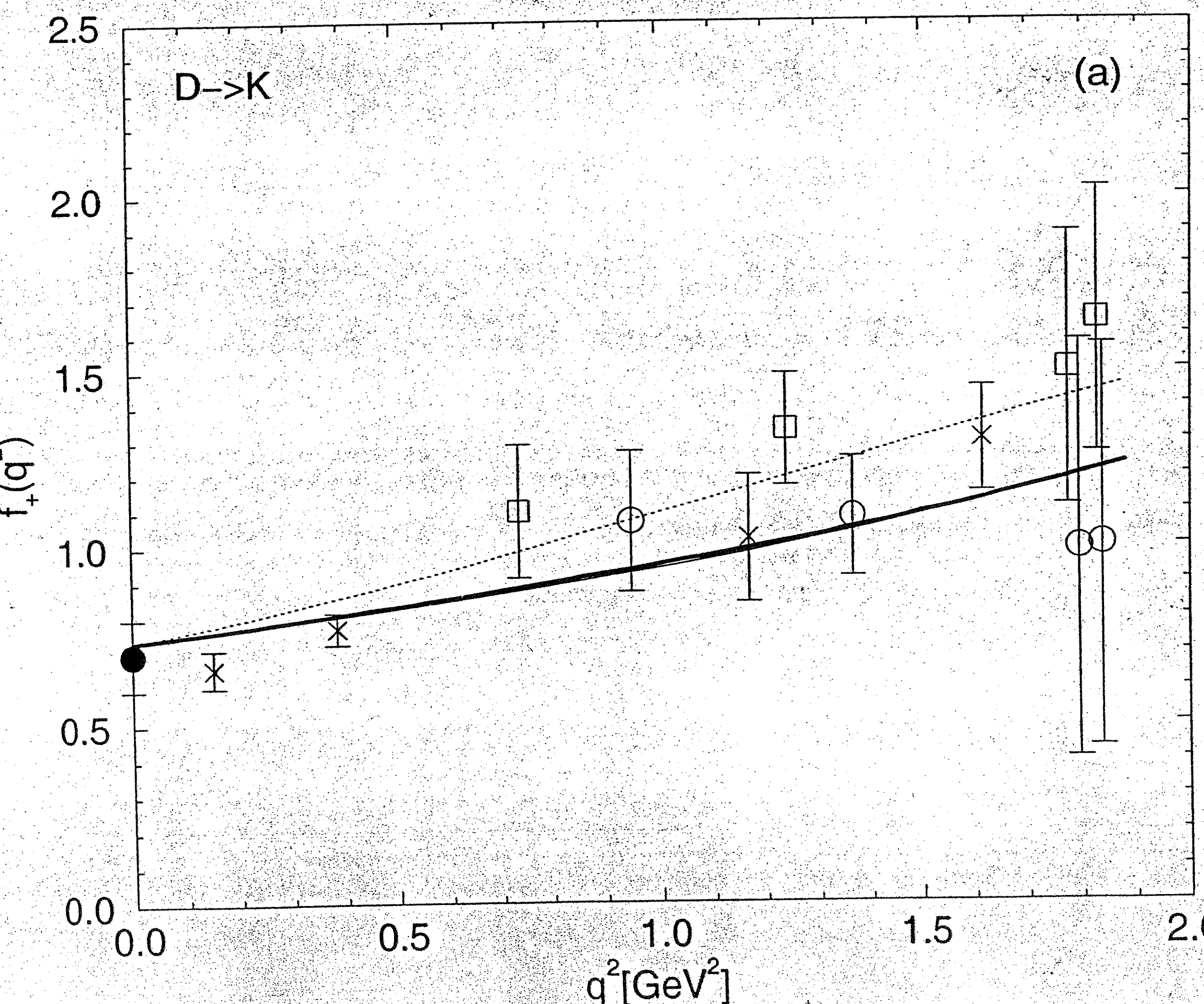

Conclusion and Discussion

1. Time-like exclusive processes require to take into account the non-wavefunction-vertex or embedded state.

2. A link has been made between the embedded state and the ordinary LF wavefunction.

3. Our results indicate that the correct implementation of the nonvalence contribution is crucial to improve the theoretical predictions for the time-like processes.

4. Although the use of constant relevant operator is encouraging for the small momentum transfer processes, the extension to include the momentum dependence should be carefully considered for the large momentum transfer processes examining the frame independence (covarian

Form Factors of Hyperons

S. Dubnička
E. Bartoš
A. Z. Dubničková

p, n
Λ
$\Sigma^+ \Sigma^0 \Sigma^-$
$\Xi^0 \; \Xi^-$

PEP-N : Measure $e^+e^- \to B\bar{B}$!

$$G_E(t) = F_1(t) + \frac{t}{4M_B^2} F_2(t)$$

$$G_M(t) = F_1(t) + F_2(t)$$

$$t = q^2 = -Q^2$$

$$\sigma(e^+e^- \to B\bar{B}) = \frac{4\pi\alpha^2}{3s} \beta_B \left[|G_M^B(s)|^2 + \frac{2M_B^2}{s} |G_E^B(s)|^2 \right)$$

$$\beta = \sqrt{1 - 4m_B^2/s}$$

Almost no data!
for $B \neq p, n$

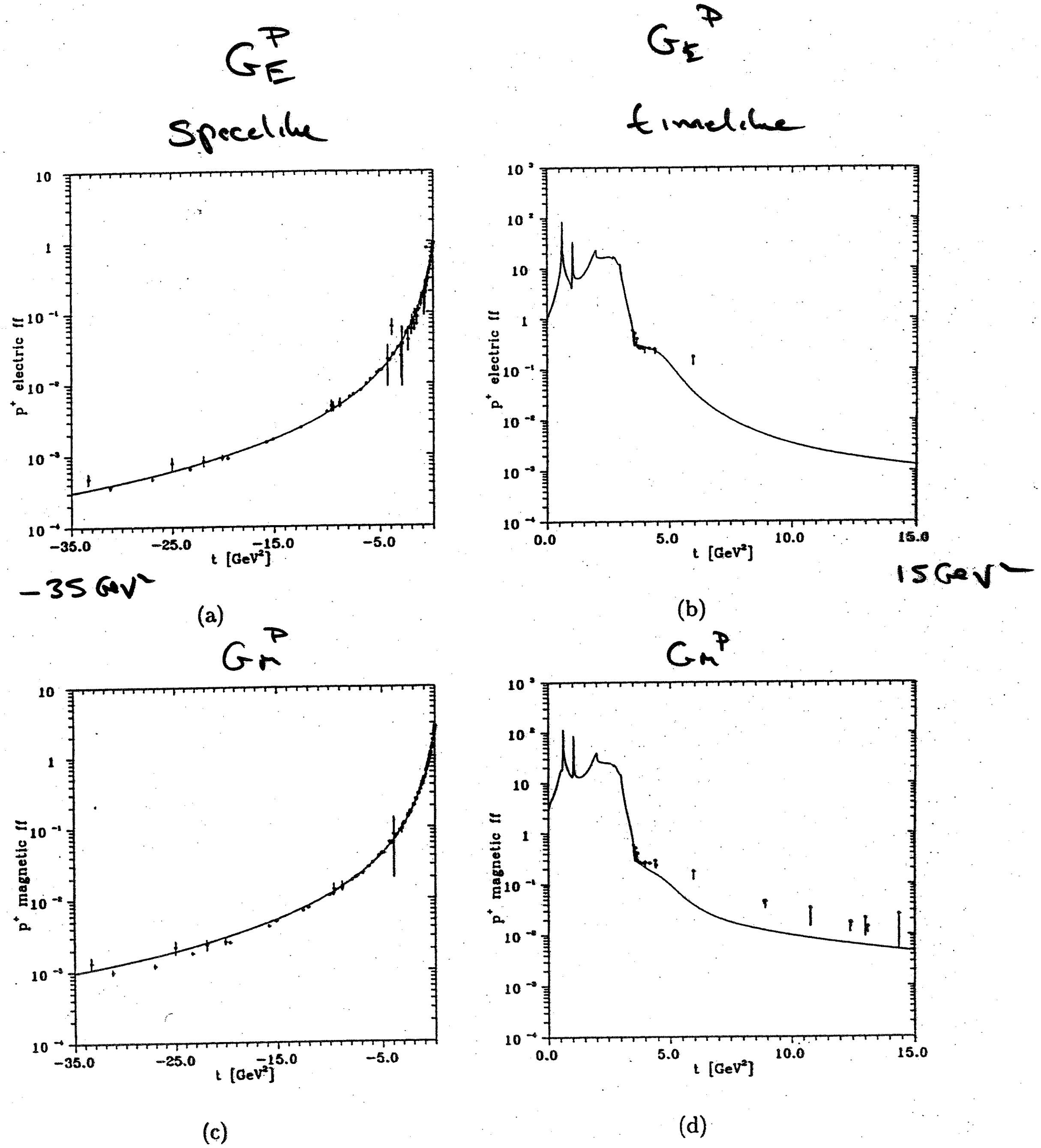

Figure 1: An optimal fit of all existing data on proton electric and magnetic FF's in space–like (left) and time–like (right) regions by the unitary and analytic nine resonance model

1

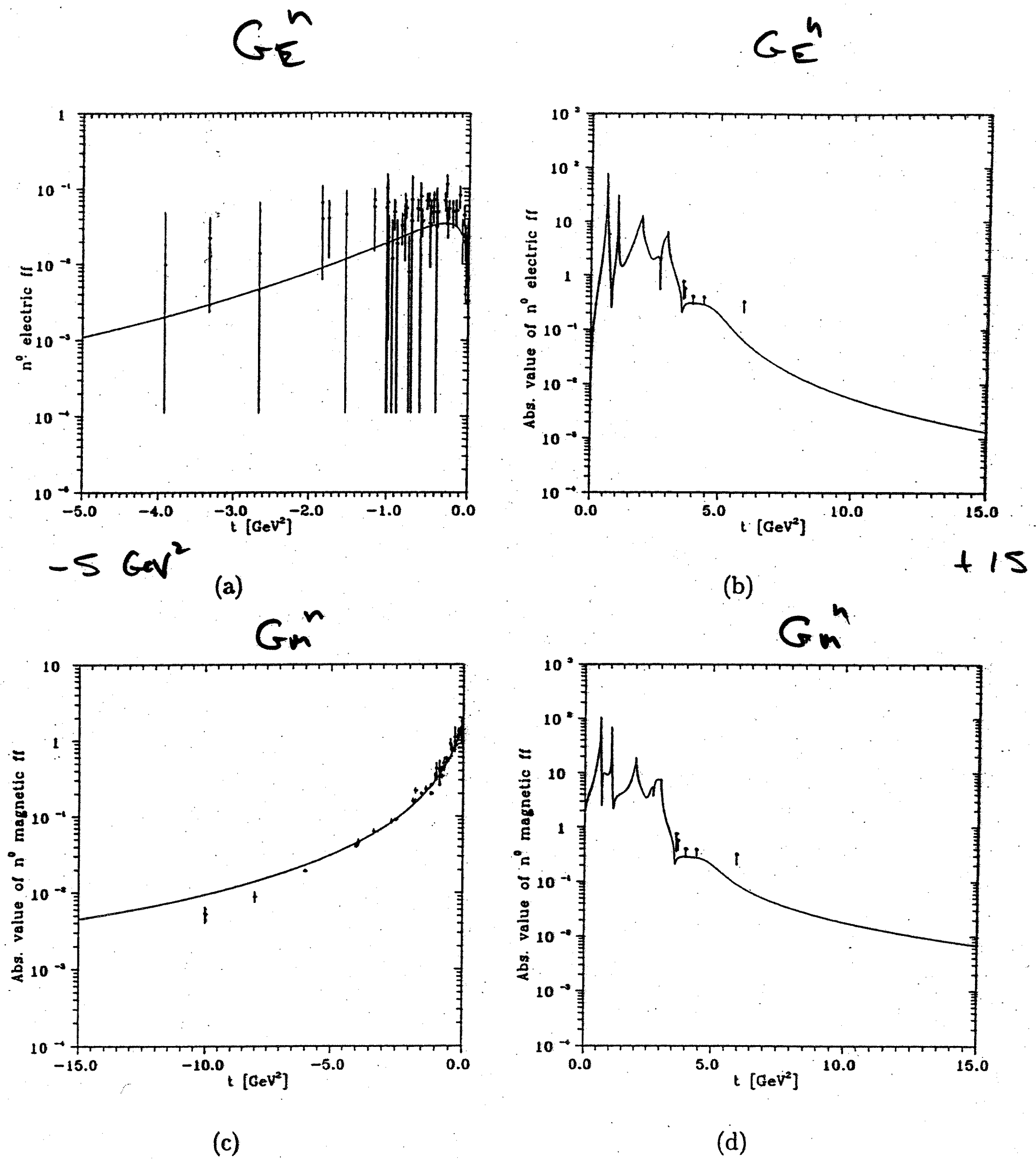

Figure 2: An optimal fit of all existing data on neutron electric and magnetic FF's in space–like (left) and time–like (right) regions by the unitary and analytic nine resonance model

Comprehensive analysis by DDB

- Normalization at $q^2=0$
- Analyticity, cut structure, hermiticity
- Schwarz reflection $F^*(t+i\epsilon) = F(t-i\epsilon)$

* Modeling:
  - vector meson resonances, widths, couplings
  - proton + neutron data
  - $SU(3)_F$

$G_E^{\Sigma^+}$

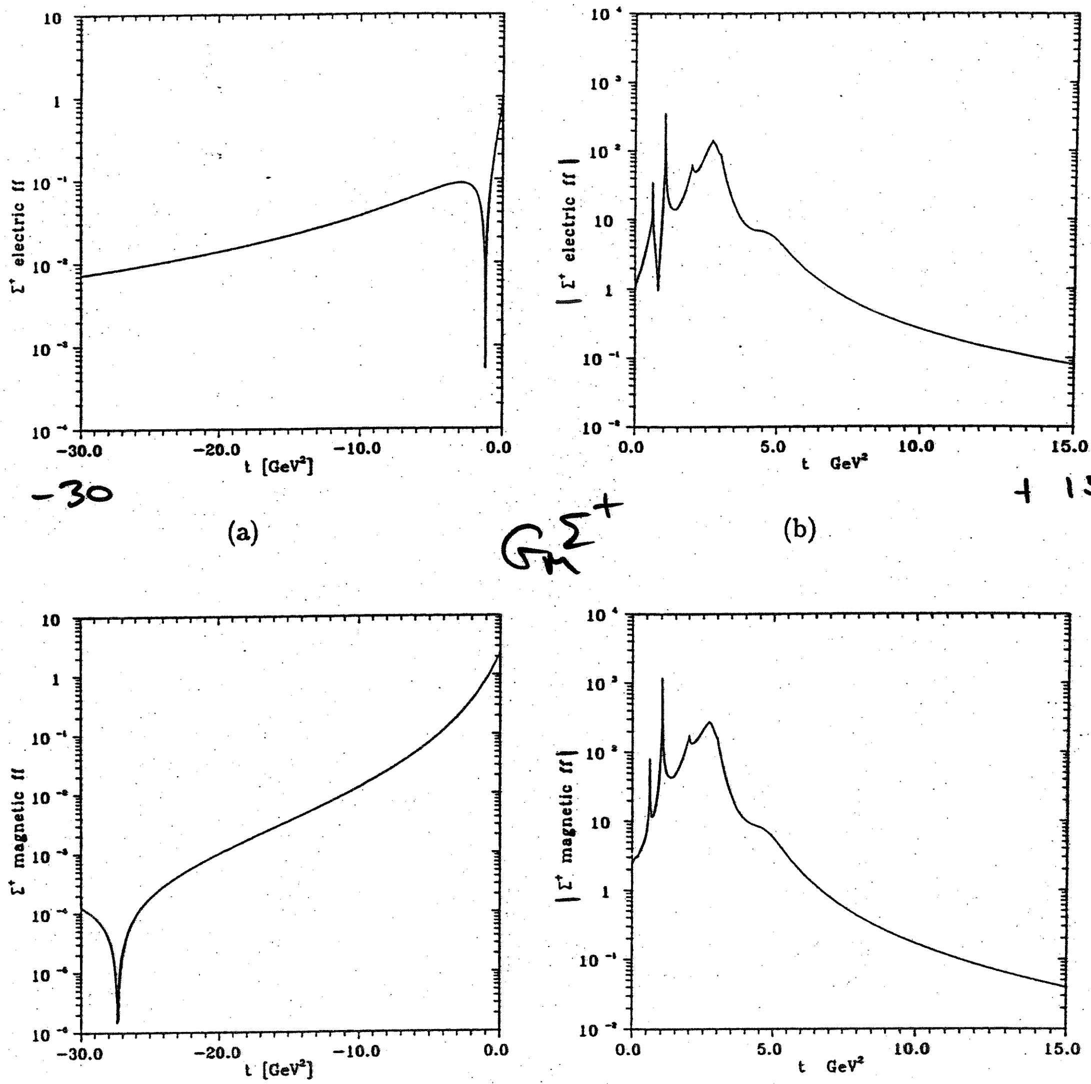

Figure 4: Predicted behaviour of Σ^+ electric and magnetic FF's in space–like (left) and time–like (right) regions by the unitary and analytic nine resonance model

Σ^0

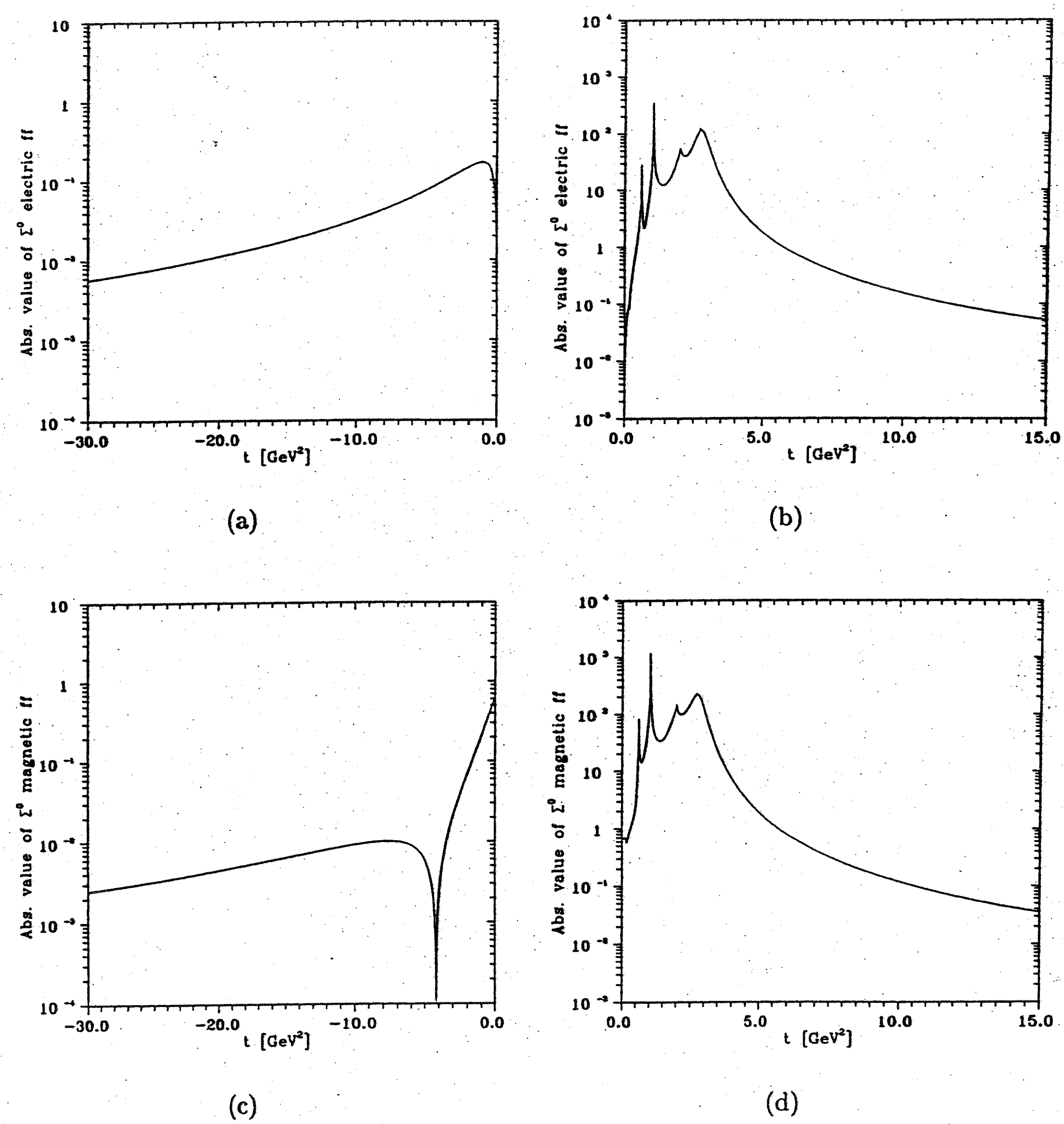

Figure 5: Predicted behaviour of Σ^0 electric and magnetic FF's in space–like (left) and time–like (right) regions by the unitary and analytic nine resonance model

18

Σ^-

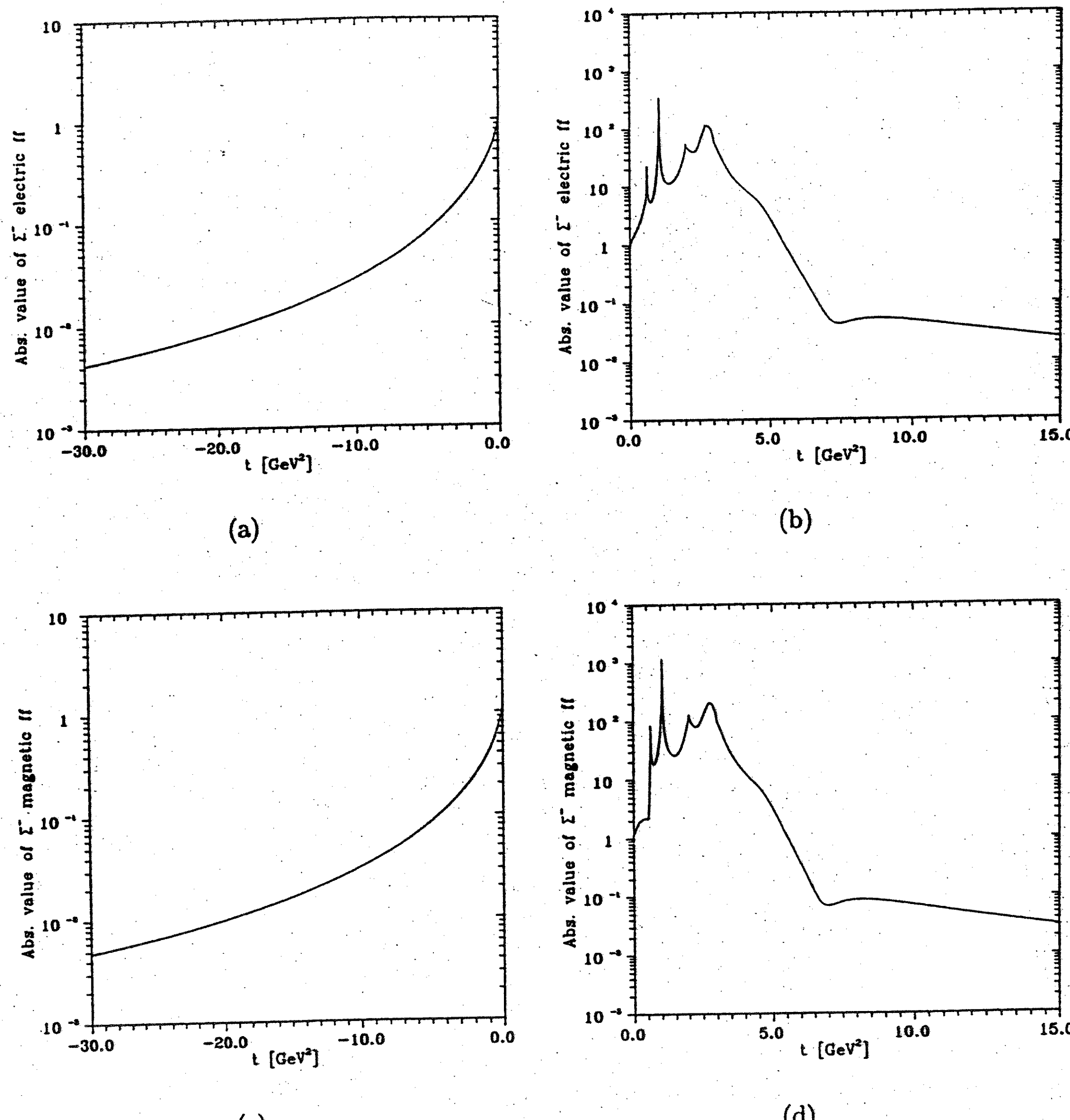

Figure 6: Predicted behaviour of Σ^- electric and magnetic FF's in space–like (left) and time–like (right) regions by the unitary and analytic nine resonance model

19

Ξ^0

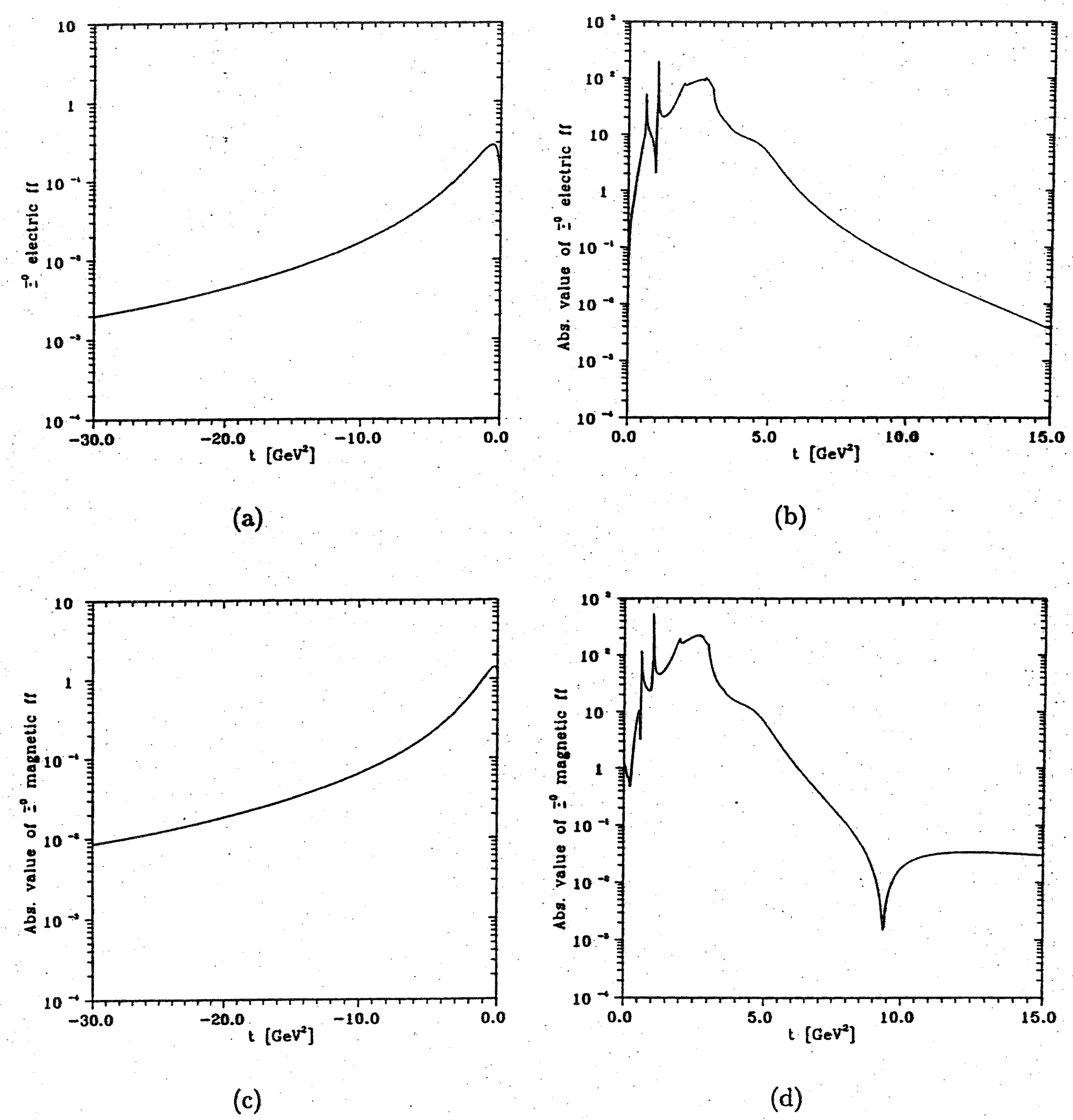

Figure 7: Predicted behaviour of Ξ^0 electric and magnetic FF's in space–like (left) and time–like (right) regions by the unitary and analytic nine resonance model

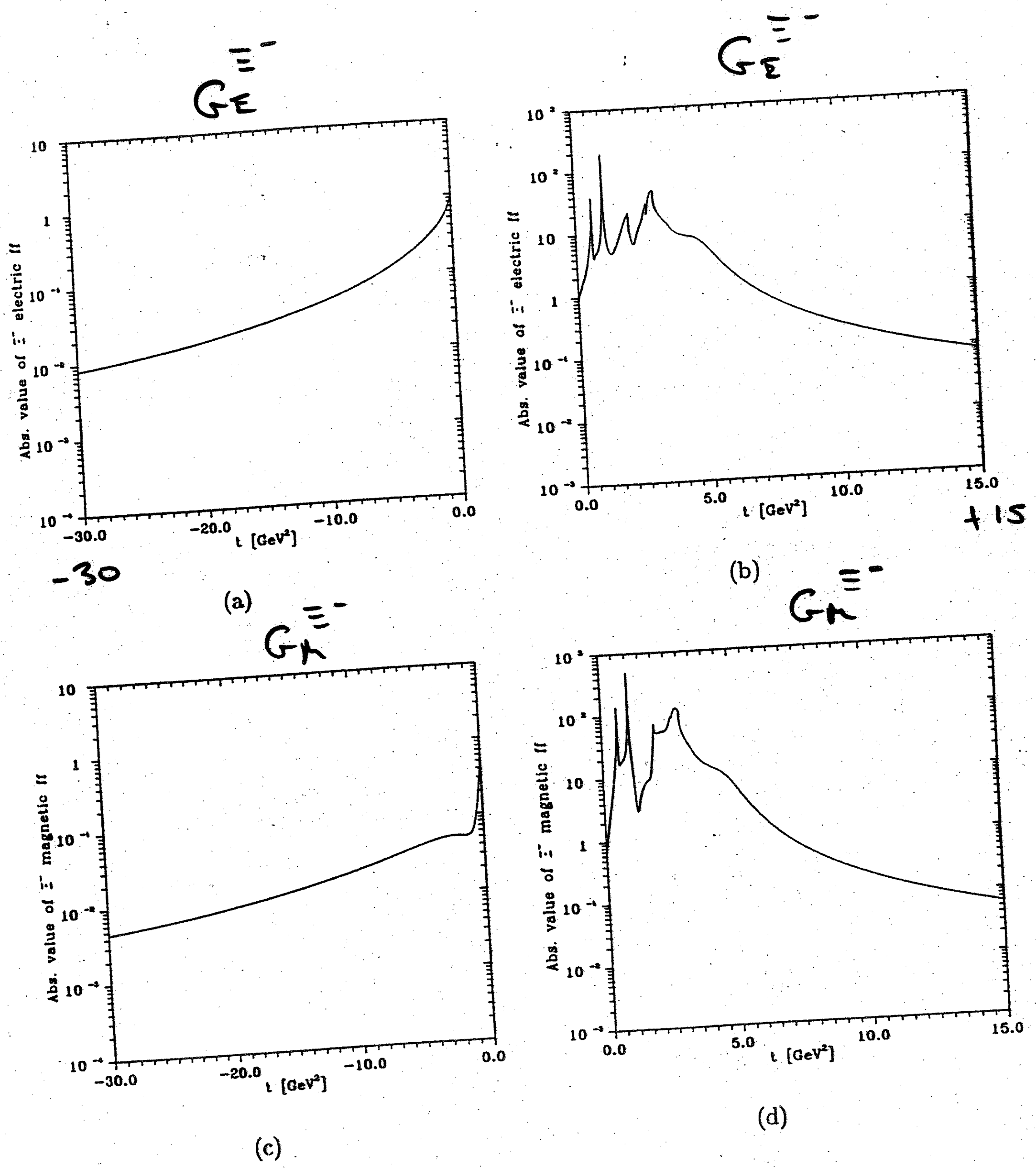

Figure 8: Predicted behaviour of Ξ^- electric and magnetic FF's in space–like (left) and time–like (right) regions by the unitary and analytic nine resonance model

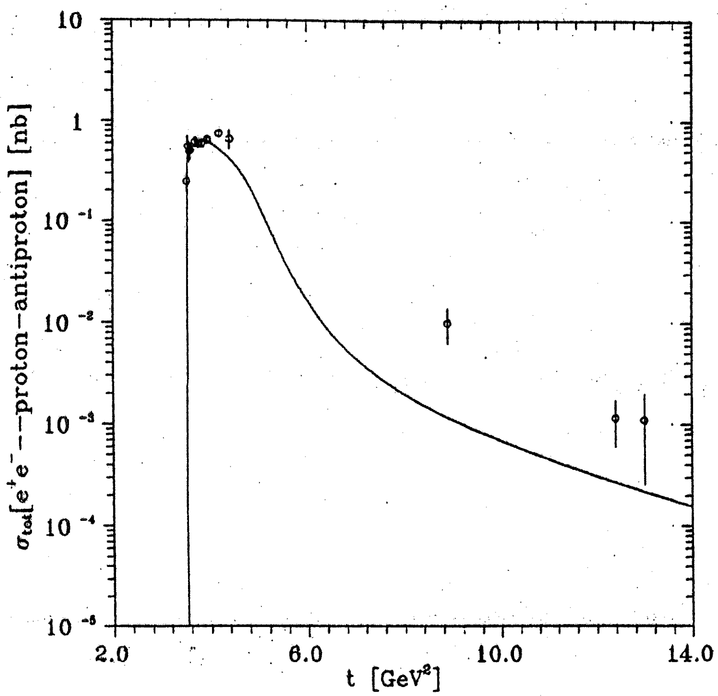

Fig.1

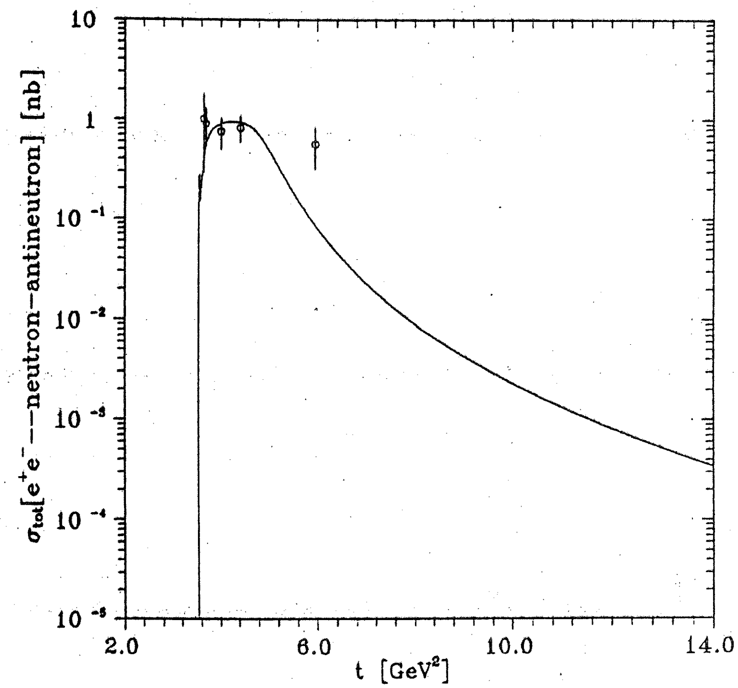

Fig.2

Fig. 9

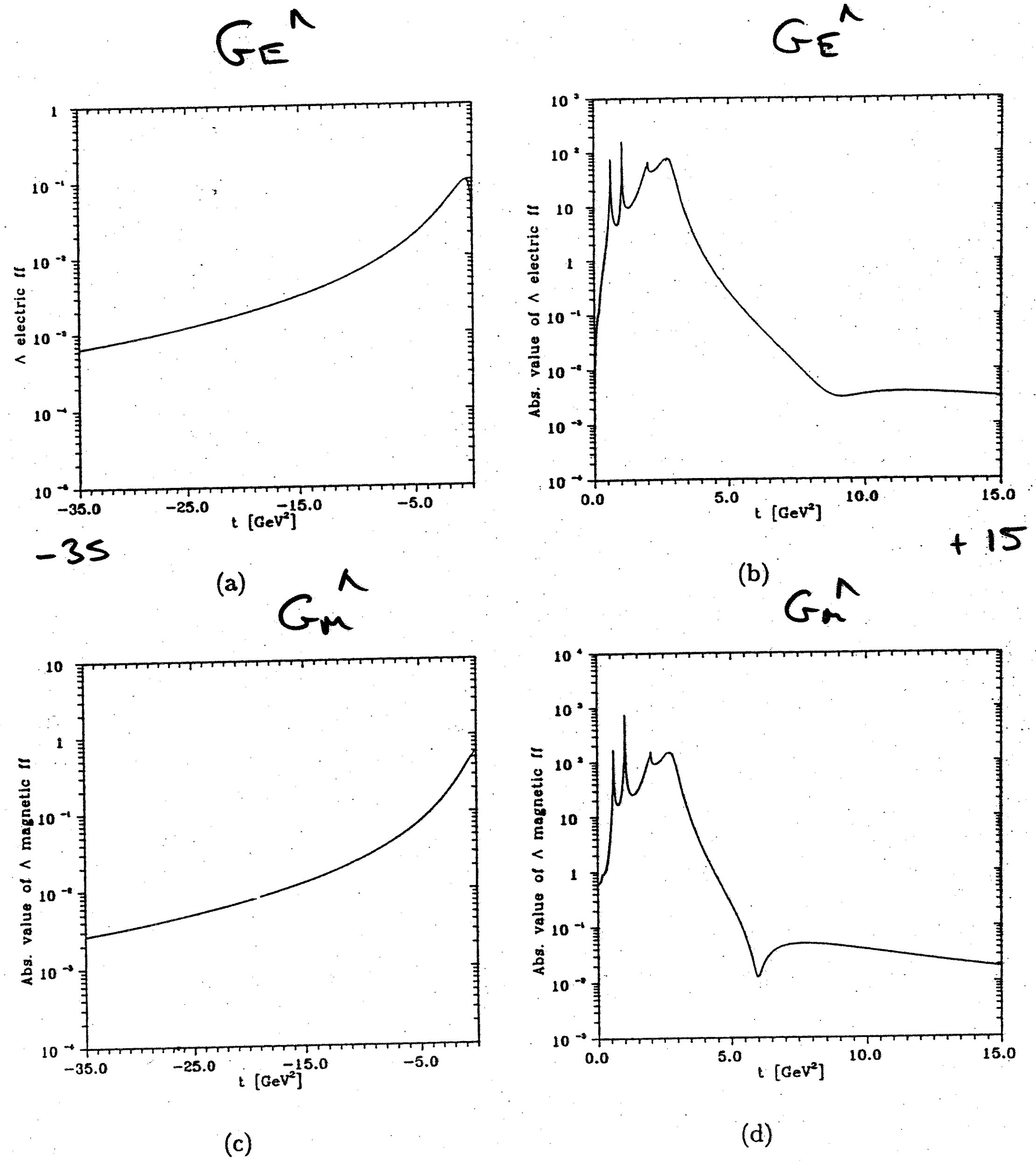

Figure 3: Predicted behaviour of Λ electric and magnetic FF's in space–like (left) and time–like (right) regions by the unitary and analytic nine resonance model

$\sigma(e^+e^- \to \Lambda\bar{\Lambda})$

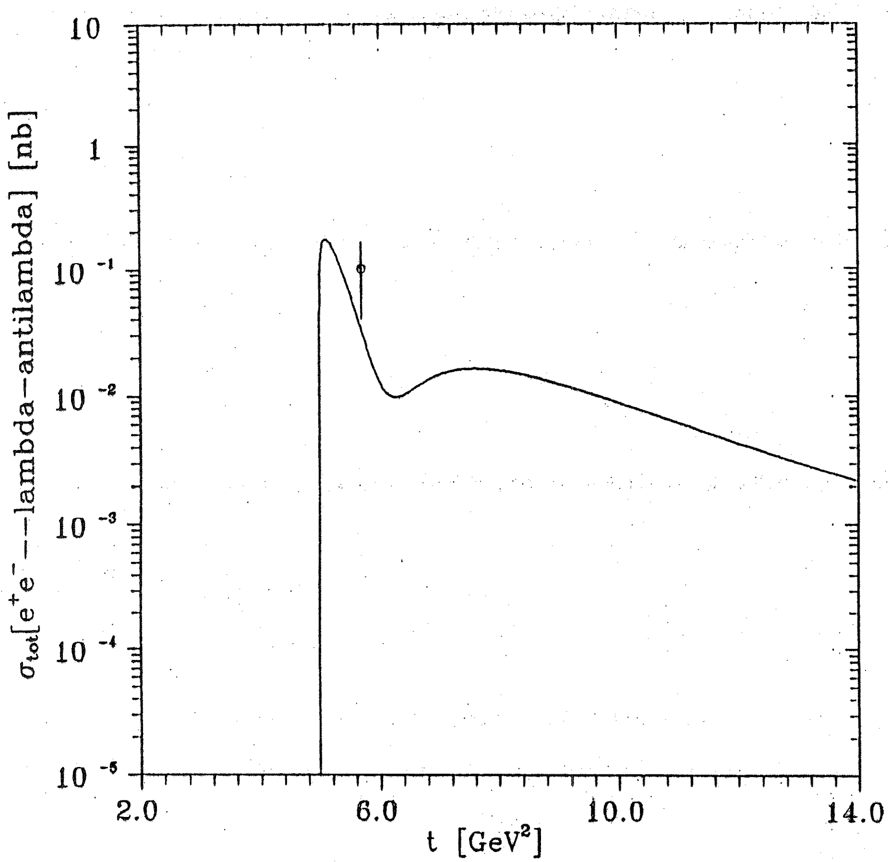

Fig.3

Fig. 10

D. C. Peaslee (U of Maryland)

* Veneziano string model (linear potential)

$m^2 = m_0^2 + N A$ radial excitations

$\rho, \rho', \rho'', \rho''', \rho^{IV}$!

$N = 1, 2, 3, 4, 5$

$q\bar{q}$ spectroscopy

$^{2S+1}L_J$ $\quad (\rho = {}^3S_1)$

$L = S, P, D$

$l = 0, 1, 2$

$\omega : I = 0$

$\rho : I = 1$

$A\langle S_1\rangle = 1.054 \pm .004$ GeV^2

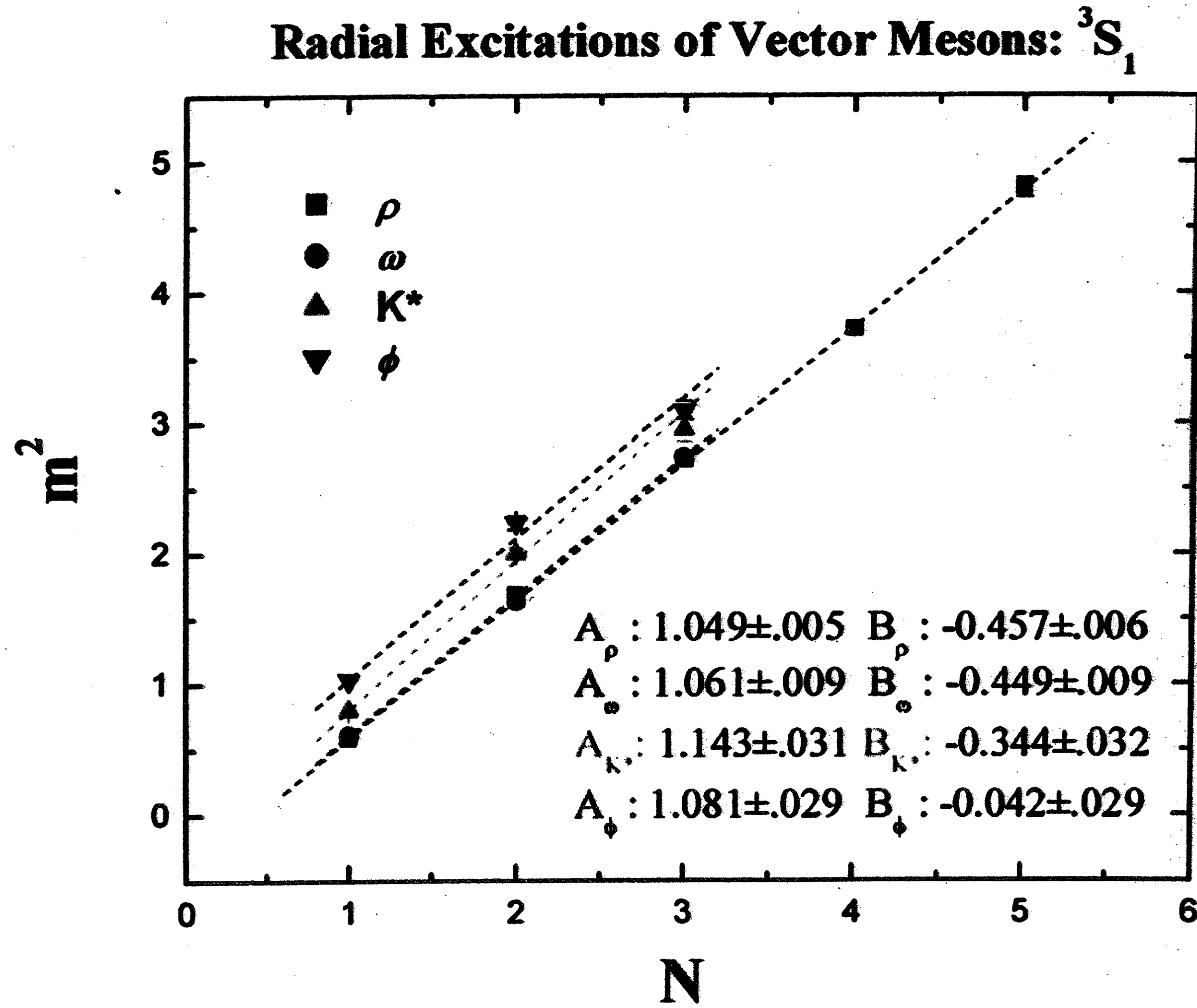

$|\Delta/\sigma| \cong .8$

$|\Delta/\sigma| \sim .7$

$|\Delta/\sigma| \sim 2.9$

$|\Delta/\sigma| \sim .9$

Radial Excitations of Vector Mesons: $^3D_1$

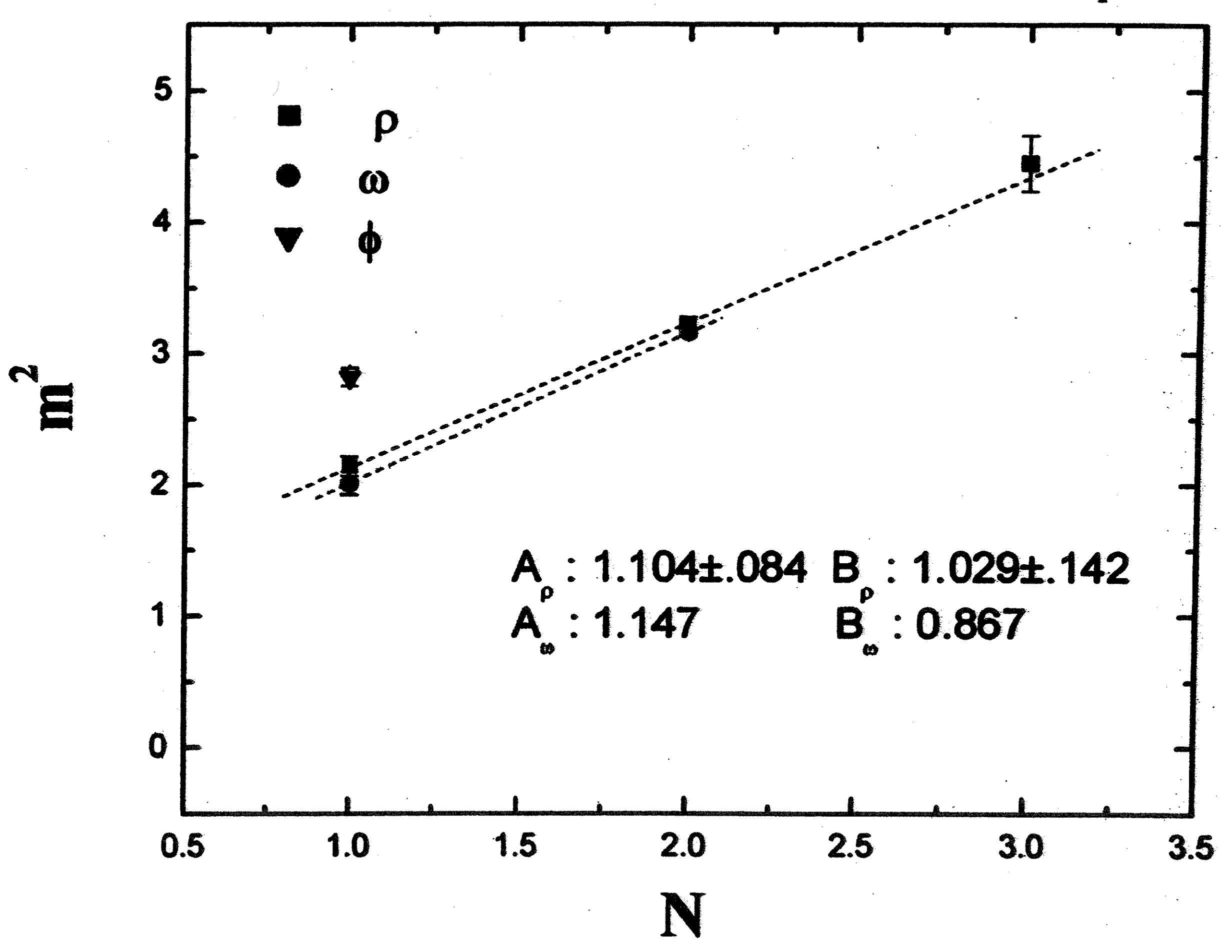

$\Delta/\sigma \sim .6$

$$m^2 = AN + B$$

$$A\{P_0, P_2, F_2\} = 1.042 \pm .006 \ \mathrm{GeV}^2$$

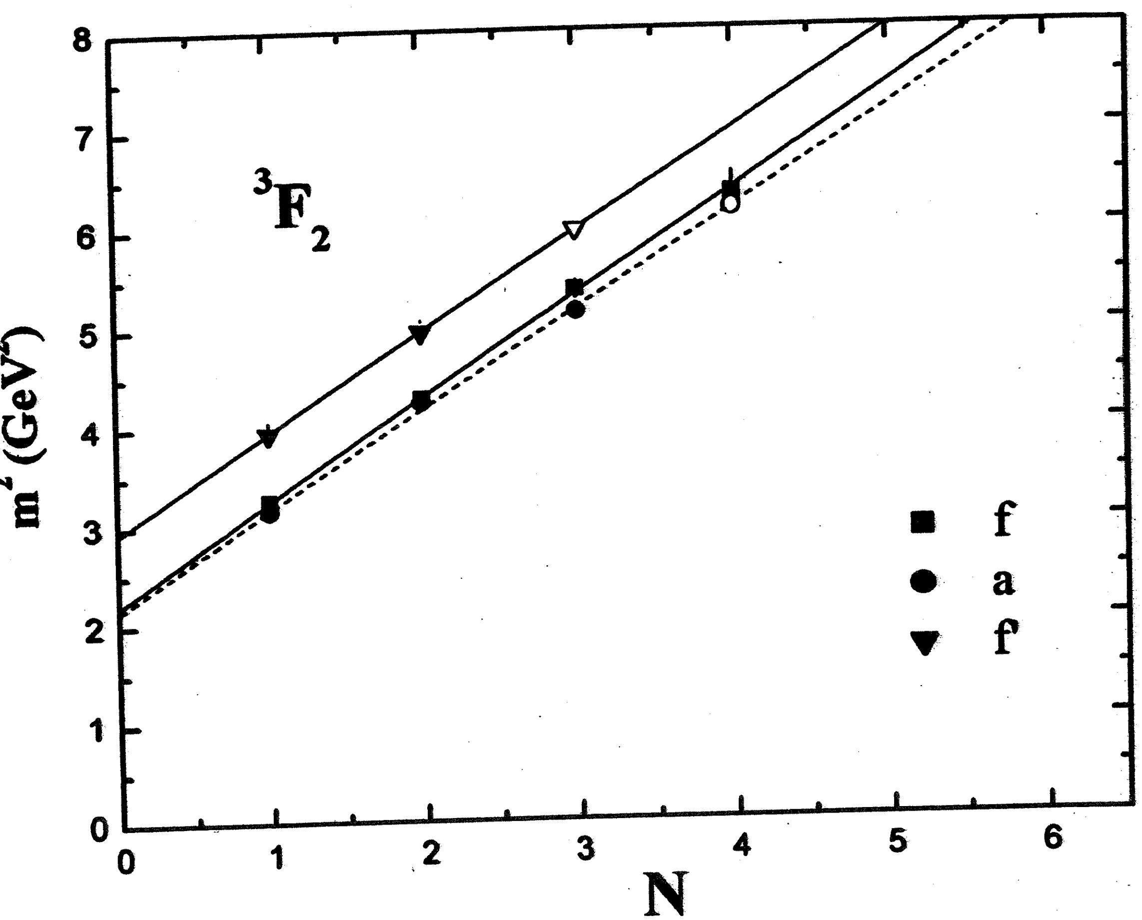

Spin 2

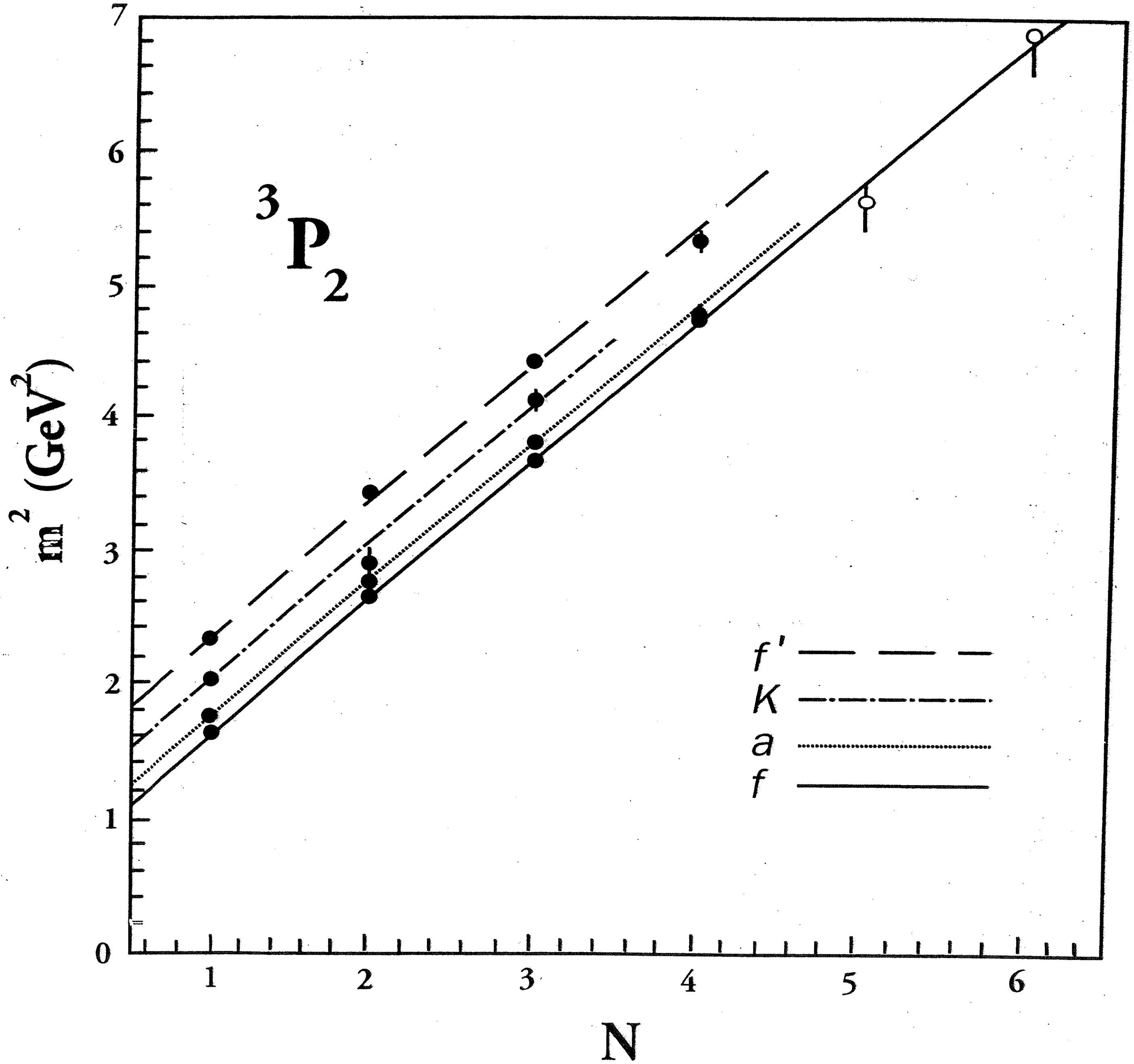

Fig. 1: Radical Trajectories for P2

C. Vogt
M. Diehl
P. Kroll

$\gamma^* \gamma^* \Rightarrow \pi^0, \eta, \eta'$

also: Ong

PEP-N : double-tagged photons

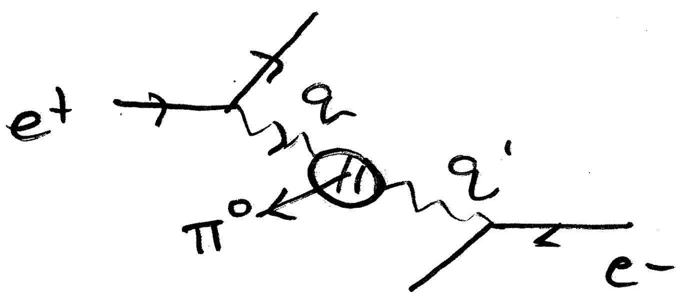

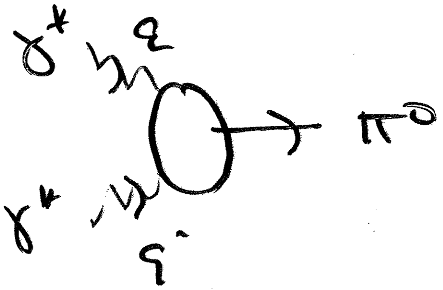

$\Rightarrow$

PQCD
leading
twist

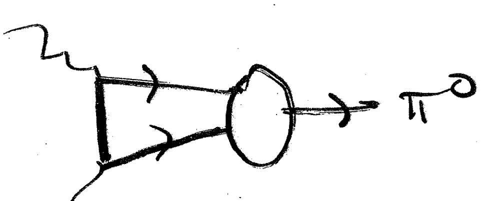

$$\bar{Q}^2 = \frac{Q^2 + Q'^2}{2}, \quad \omega = \frac{Q^2 - Q'^2}{Q^2 + Q'^2}$$

The $\pi - \gamma^*$–transition form factor

- Definition of transition form factor through $\gamma^*\gamma^*\pi$-vertex:

$$\Gamma_{\mu\nu} = -ie_0^2\, F_{\pi\gamma^*}(Q^2, Q'^2)\, \varepsilon_{\mu\nu\alpha\beta}\, q_1^\alpha q_2^\beta\,,$$

- Convenient variables:

$$\overline{Q}^2 = \frac{Q^2 + Q'^2}{2}, \quad \omega = \frac{Q^2 - Q'^2}{Q^2 + Q'^2}$$

- Born diagrams contributing to $F_{\pi\gamma^{(*)}}$:

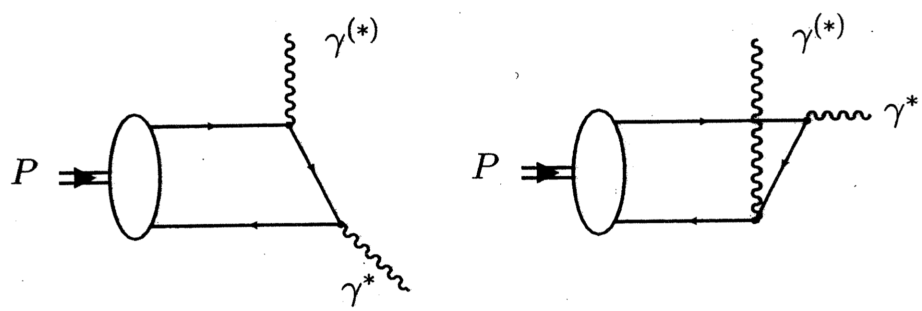

- Leading twist, NLO α_s-expression in hard scattering approach [Brodsky, Lepage, 1980]:

$$F_{\pi\gamma^*}(\overline{Q}, \omega) = \frac{1}{3\sqrt{2}}\,\frac{f_\pi}{\overline{Q}^2}\int_{-1}^{1} d\xi\, \frac{\Phi_\pi(\xi, \mu_F)}{1+\xi\omega}\left[1 + \frac{\alpha_s(\mu_R)}{\pi}\,\mathcal{K}(\omega, \xi)\right]$$

Properties of the pion distribution amplitude

- Relation of pion DA Φ_π to pion's light-cone wave function:
  [Brodsky, Lepage, 1980]
  $$\Phi_\pi(\xi;\mu_F) \sim \int^{\mu_F^2} [d^2k_\perp]\, \Psi_\pi(\xi, \mathbf{k}_\perp)$$
  $\xi = 2x - 1$, x usual light-cone momentum fraction
- Φ_π describes distribution of pion's longitudinal momentum among its (partonic) constituents.
- Only lowest Fock state contributions to hard scattering reactions at leading order pQCD.
- Normalization of $q\bar{q}$-Fock state wave function from $\pi^+ \to \mu^+\nu_\mu$:
  $$\frac{4\pi f_\pi}{\sqrt{6}} = \int_{-1}^{1} d\xi\, \hat{\Psi}_\pi(\xi, b_\perp = 0)$$
  "wave function at origin of transverse configuration space"
- Solution of evolution equation in terms of expansion upon Gegenbauer polynomials $C_n^{3/2}$:
  $$\Phi_\pi(\xi,\mu_F) = \Phi_{\rm AS}(\xi)\left[1 + \sum_{n=2,4,\ldots}^{\infty} B_n^\pi(\mu_F)\, C_n^{3/2}(\xi)\right]$$
- B_n^π Gegenbauer coefficients:
  $$B_n^\pi(\mu_F) = B_n^\pi(\mu_0)\left(\frac{\alpha_s(\mu_F)}{\alpha_s(\mu_0)}\right)^{\gamma_n}$$
- Asymptotic form of pion DA:
  $$\Phi_{\rm AS}(\xi) = \frac{3}{2}(1-\xi^2)$$

The $\pi - \gamma^*$–transition form factor

- Rewrite using Gegenbauer expansion:

$$F_{\pi\gamma^*}(\overline{Q},\omega) = \frac{f_\pi}{\sqrt{2}\,\overline{Q}^2} \sum_{n=0,2,\ldots} C_n(\omega)\, B_n^\pi(\mu_F)$$

with analytically computable functions $C_n(\omega)$

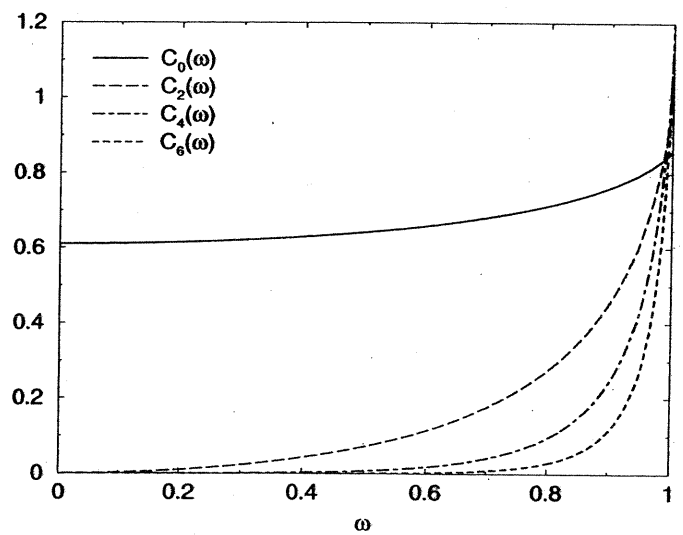

- Sensitive to Gegenbauer coefficients B_n^π only for $\omega \to 1$, i.e., for one photon being nearly on-shell.

The $\pi - \gamma^*$–transition form factor

- In the limit $\omega \to 1: \ C_n(\omega) \to 1 + \mathcal{O}(\alpha_s)$:
  case of transition form factor for *real* photons.
- In that case, form factor measures $(1+\xi)^{-1}$-moment, given by sum over all Gegenbauer coefficients:

$$\langle (1+\xi)^{-1} \rangle = \frac{3}{2}[1 + \sum_n B_n^\pi(\mu_F)]$$

- From phenomenological analysis of CLEO data: [Kroll, Raulfs, 1996]

$$\langle (1+\xi)^{-1} \rangle = 1.37 \quad \text{at} \quad Q^2 = 8\,\mathrm{GeV}^2$$

- Consequence for pion DA, e.g. $B_n^\pi = 0$ for $n \geq 4$:

$$B_2^\pi(\mu_0 = 0.5\,\mathrm{GeV}) = -0.15$$

$\rightsquigarrow$ pion DA is close to asymptotic form

[Musatov, Radyushkin, 1997; Brodsky, Ji, Pang, Robertson, 1998]

The $\pi - \gamma^*$–transition form factor

- Small sensitivity w.r.t. B_n^π follows from fast decrease of $C_n(\omega)$ for $\omega \to 0$: expansion in powers of ω:

$$\begin{aligned} F_{\pi\gamma^*}(\overline{Q},\omega) &= \frac{\sqrt{2}f_\pi}{3\,\overline{Q}^2}\Big[1 - \frac{\alpha_s(\overline{Q})}{\pi} + \frac{1}{5}\,\omega^2\Big(1 - \frac{5}{3}\frac{\alpha_s(\overline{Q})}{\pi}\Big) \\ &+ \frac{12}{35}\,\omega^2 B_2^\pi(\overline{Q})\Big(1 + \frac{5}{12}\frac{\alpha_s(\overline{Q})}{\pi}\Big)\Big] + \mathcal{O}(\omega^4, \alpha_s^2) \end{aligned}$$

- First appearance of B_n^π at order ω^n
- $\leadsto$ Extraction of B_n^π from $\gamma^* \to \pi$-form factor difficult.
- But: parameter-free prediction of pQCD to leading twist accuracy for $\omega \to 0$: [Cornwall, 1966; Köpp, Walsh, Zerwas, 1974]

$$\overline{Q}^2 F_{\pi\gamma^*}(\overline{Q},\omega) = \frac{\sqrt{2}f_\pi}{3}\Big[1 - \frac{\alpha_s(\overline{Q})}{\pi}\Big]$$

valid over a wide range of ω !

- Any deviation from this prediction would signal power corrections !

The $\pi - \gamma^*$–transition form factor

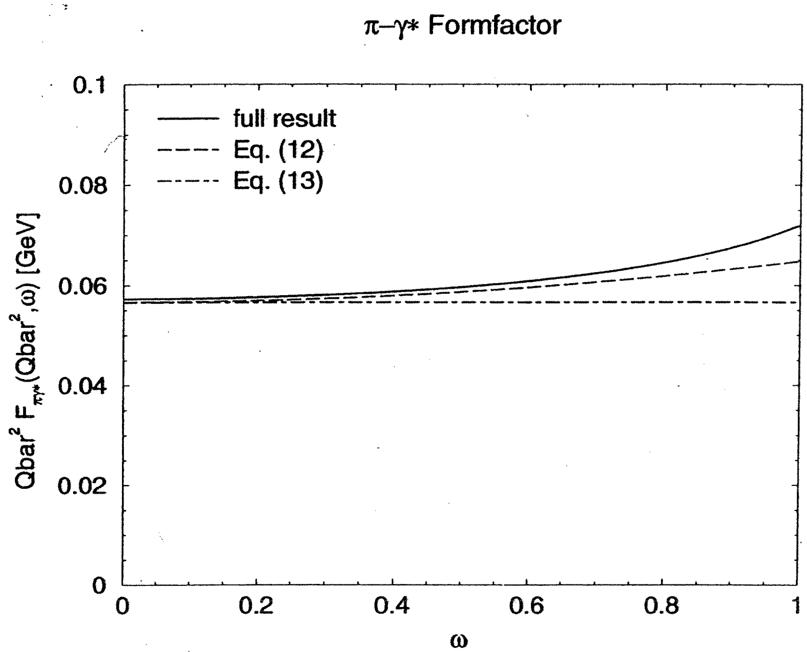

Is $\omega = 1$
at CLEO?
Need anti-Tag

The $\pi - \gamma^*$–transition form factor

- Complication in the limit $\omega \to 1$: sensitivity to endpoint regions, $\xi \to \pm 1$.
- Large power corrections may spoil accuracy of data analysis.
- Investigation of partonic transverse momentum and Sudakov corrections within modified hard scattering approach:

  [Botts, Li, Sterman, 1989, 1992]

$$
\begin{aligned}
F_{\pi\gamma^*}(\overline{Q}, \omega) &= \frac{1}{4\sqrt{3}\pi^2} \int d\xi \, d^2\mathbf{b} \, \hat{\Psi}^*_\pi(\xi, -\mathbf{b}, \mu_F) \\
&\times \; K_0(\sqrt{1 + \xi\omega}\, \overline{Q}\, b) \, \exp\left[-S\left(\xi, b, \overline{Q}, \mu_R\right)\right]
\end{aligned}
$$

b Fourier conjugate to $\mathbf{k}_\perp$ $a_{tr}^2 = \frac{1}{8\pi^2 f^2}$

- Asymptotically, only small transverse $q\bar{q}$-separations survive due to behaviour of Sudakov factor.
- Example: Gaussian ansatz

$$
\hat{\Psi}^\pi_{\rm AS}(\xi, \mathbf{b}) = \frac{2\pi f_\pi}{\sqrt{6}} \, \Phi_{\rm AS}(\xi) \, \exp\left[-\frac{\pi^2}{2} f_\pi^2 \left(1 - \xi^2\right) b^2\right]
$$

The $\pi - \gamma^*$–transition form factor

- Ratio of transition form factor in modified / collinear approach

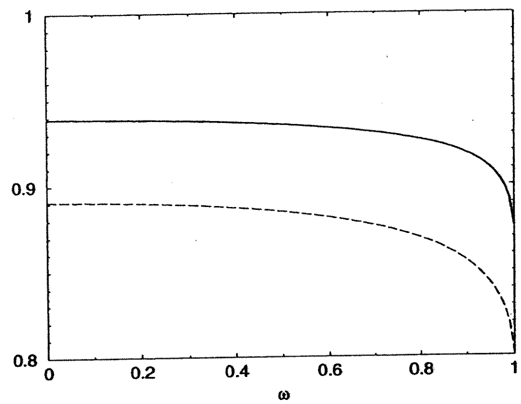

- dashed line: $\overline{Q}^2 = 2\,\mathrm{GeV}^2$, solid line: $\overline{Q}^2 = 4\,\mathrm{GeV}^2$.
- $\mathbf{k}_\perp$-corrections negligible for $\overline{Q}^2 \gtrsim 4\,\mathrm{GeV}^2$ and $\omega \lesssim 0.9$: domination of leading twist.
- However, small sensitivity to coefficients B_n^π in this region.

The case of the eta

- Analogous discussion for $\gamma^* \to \eta,\ \eta'$ transitions.
- Complication through $\eta - \eta'$ mixing and contributions from gluon DA at $\mathcal{O}(\alpha_s)$.

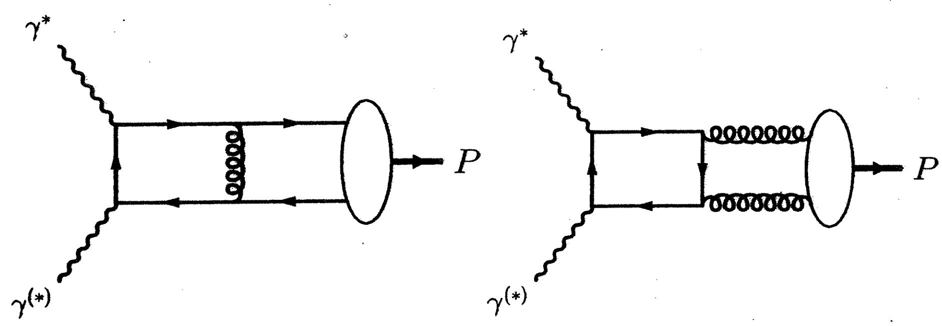

- Convenient: Fock state decomposition with $\mathrm{SU}(3)_\mathrm{F}$ singlet and octet valence quark states: $(P = \eta,\ \eta')$

$$
\begin{aligned}
\mid P\rangle \;&=\; \frac{f_P^{(8)}}{2\sqrt{6}}\Phi_P^{(8)}(\xi) \mid (\mathrm{u\bar{u}} + \mathrm{d\bar{d}} - 2\mathrm{s\bar{s}})/\sqrt{6}\rangle \\
&+\; \frac{f_P^{(1)}}{2\sqrt{6}}\left[\Phi_P^{(1)}(\xi) \mid (\mathrm{u\bar{u}} + \mathrm{d\bar{d}} + \mathrm{s\bar{s}})/\sqrt{3}\rangle + \Phi_P^{(\mathrm{g})}(\xi) \mid \mathrm{gg}\rangle\right] + \ldots
\end{aligned}
$$

- Definition of decay constants:

$$
\langle 0 \mid J_{\mu 5}^{(i)} \mid P(p)\rangle = i f_P^{(i)} p_\mu, \qquad (i = 1, 8)
$$

The case of the eta

- Singlet quark and gluon DAs:

$$\begin{aligned}\Phi_P^{(1)}(\xi,\mu_F) &= \Phi_{\rm AS}(\xi)\Big\{1 \\ &+ \sum_{n=2,4,\ldots}^{\infty}\Big[B_{Pn}^{(1)}(\mu_F)+\rho_n^{(g)}B_{Pn}^{(g)}(\mu_F)\Big]\,C_n^{3/2}(\xi)\Big\} \\ \Phi_P^{(g)}(\xi,\mu_F) &= \frac{(1-\xi^2)^2}{16}\sum_{n=2,4,\ldots}^{\infty}\Big[\rho_n^{(1)}B_{Pn}^{(1)}(\mu_F)+B_{Pn}^{(g)}(\mu_F)\Big]\,C_{n-1}^{5/2}(\xi)\end{aligned}$$

- Similar expansion in ω and Gegenbauer polynomials:

$$\begin{aligned}F_{P\gamma^*}(\overline{Q},\omega) &= \frac{\sqrt{2}\,f_P^{\rm eff}}{3\,\overline{Q}^2}\Big\{1-\frac{\alpha_s(\mu_R)}{\pi}+\frac{1}{5}\,\omega^2(1-\frac{5}{3}\frac{\alpha_s(\mu_R)}{\pi}) \\ &+ \frac{12}{35}\frac{\omega^2}{\sqrt{3}\,f_P^{\rm eff}}\big[f_P^{(8)}B_{P2}^{(8)}+2\sqrt{2}f_P^{(1)}(B_{P2}^{(1)}+\rho_2^{(g)}B_{P2}^{(g)})\big] \\ &\times \Big[1+\frac{5}{12}(1+\frac{10}{3}\ln 2)\frac{\alpha_s(\mu_R)}{\pi}\Big] \\ &+ \frac{10}{189}\frac{f_P^{(1)}}{\sqrt{3}\,f_P^{\rm eff}}\,\omega^2(\rho_2^{(1)}B_{P2}^{(1)}+B_{P2}^{(g)})\frac{\alpha_s(\mu_R)}{\pi}\Big\}+\mathcal{O}(\omega^4,\alpha_s^2)\end{aligned}$$

with effective decay constants $f_P^{\rm eff}=\frac{1}{\sqrt{3}}[f_P^{(8)}+2\sqrt{2}f_P^{(1)}]$

- Gluon contributions amount to few percent.
- Again: small sensitivity to Gegenbauer coefficients.

Summary

- Meson DAs important, universal objects in hard exclusive reactions, which embody soft physics.
- Form factor for transitions $\gamma \to P$ measures sum of expansion coefficients.
- Form factor for transitions $\gamma^* \to P$ independent of DA's shape over wide kinematical region.
- $\rightsquigarrow$ Parameter-free, leading twist prediction of pQCD, deserves experimental verification !

Hadron Production at Intermediate Energies and Lund Area Law

Haiming Hu
Institute of High Energy Physics
CAS Beijing
huhm@pony1.ihep.ac.cn
huhm@hpws4.ihep.ac.cn

May 1, 2001

Hai-Ming Hu (ITEP)

Hadronization in Low Energy e^+e^-
- Lund String Model

$\Rightarrow$ Direct application to PEP-N, ..

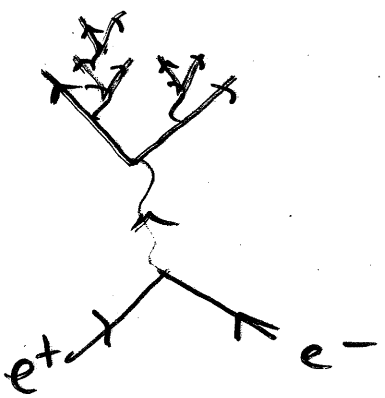

$$f(z) = \frac{N}{z}(1-z)^a e^{-\frac{bm^2}{z}}$$

Remarkable fit
to
$e^+e^- \to X$ data
$\sqrt{s} > 2.4$ GeV

* Central principle of Lund model

Area law of Hadronization

Probability of Fracture e^{-bA}

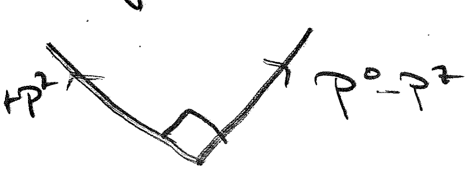

Fractal
Structure

Frame + stage-independent

Lund string fragmentation hadronization

The hadron production picture is that string fragmentation by a **set of new pairs** $(q\bar{q})$ and $(q\bar{q}q\bar{q})$ production, **hadrons form at vertices**.

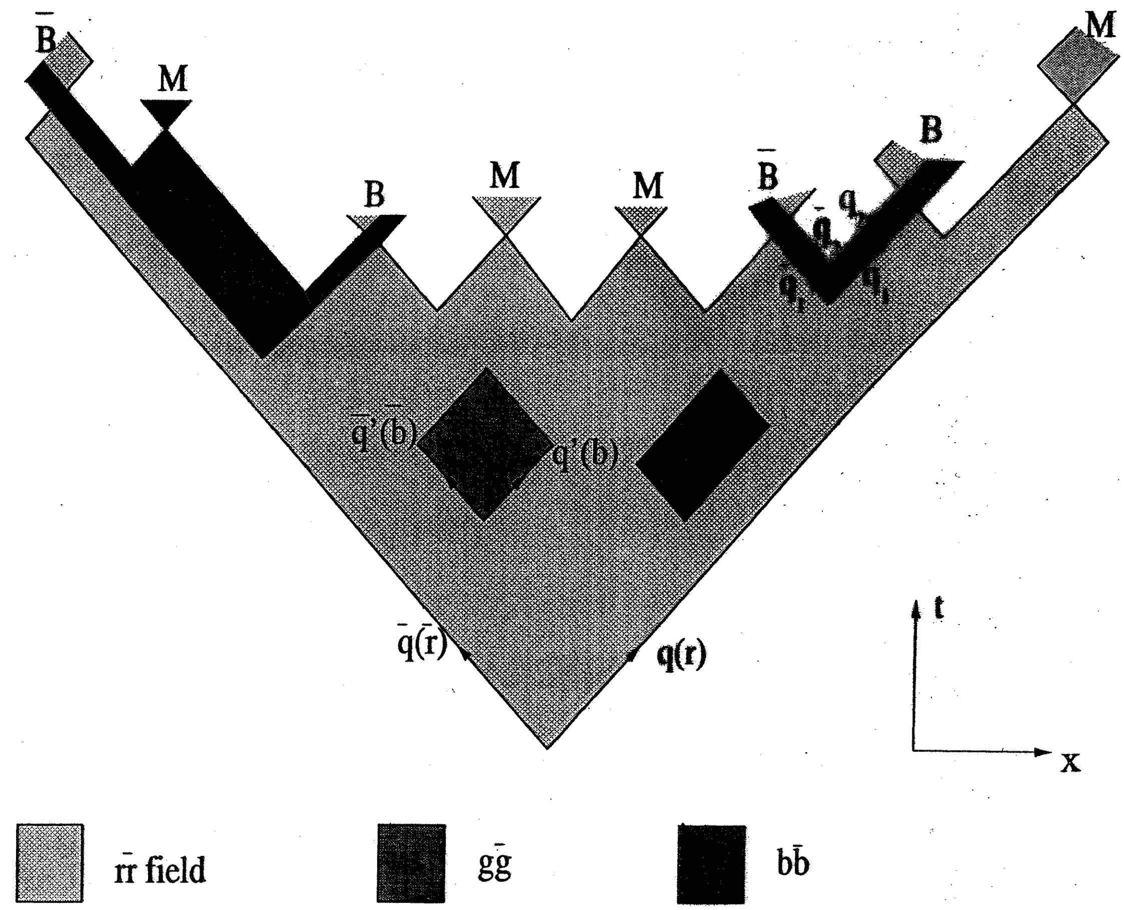

Figure 1: *String fragmentation in $t-x$ space. The produced new pairs $(q\bar{q})$ and $(q\bar{q}q\bar{q})$ may form mesons and baryons if they carry with the correct flavor quantum number, othewise they just behave like the vacuum fluctuations and do not lead any observable effects in experiments.*

Derivation of the area law

Lund string fragmentation process is Lorentz invariant and factorization. The finite energy (s) system containing n hadrons may be viewed as a part of infinite system with energy $s_0 \to \infty$.

The processes occurring in **subsystem is the same** as it be a complete system starting at the some original energy s.

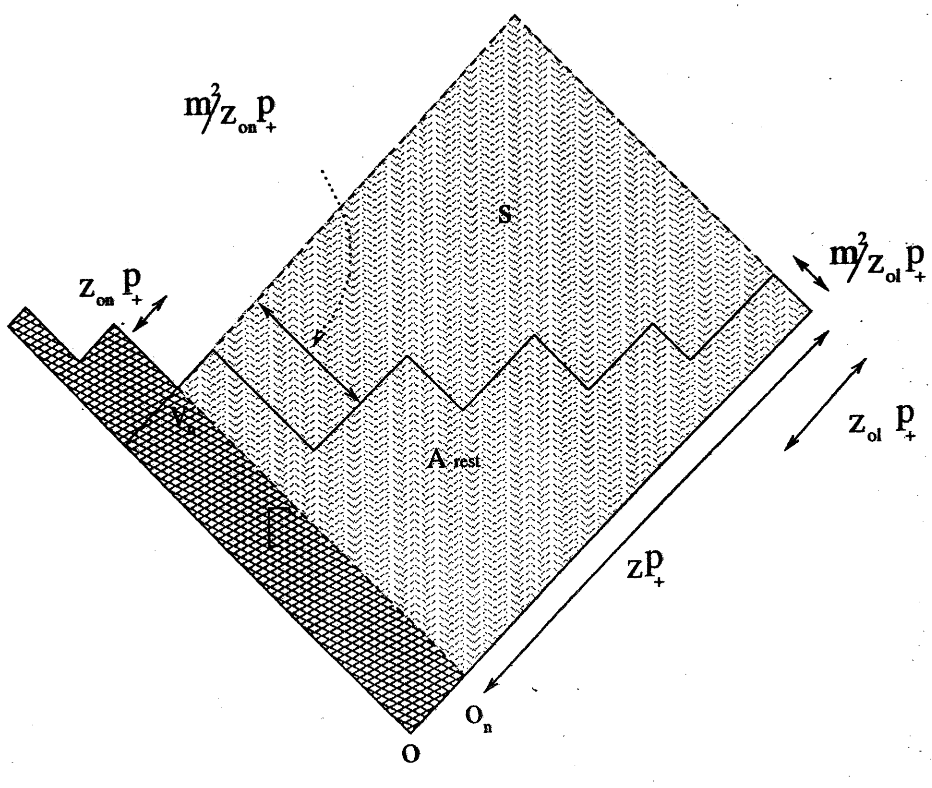

Figure 2: *The situation after n steps fragmentation. s is the squared invariant mass of the n-hadrons subsystem, $\mathcal{A}_{rest} = \mathcal{A}_n$ is the area enclosed by the quark and antiquark light-cone momentum lines of n particles.*

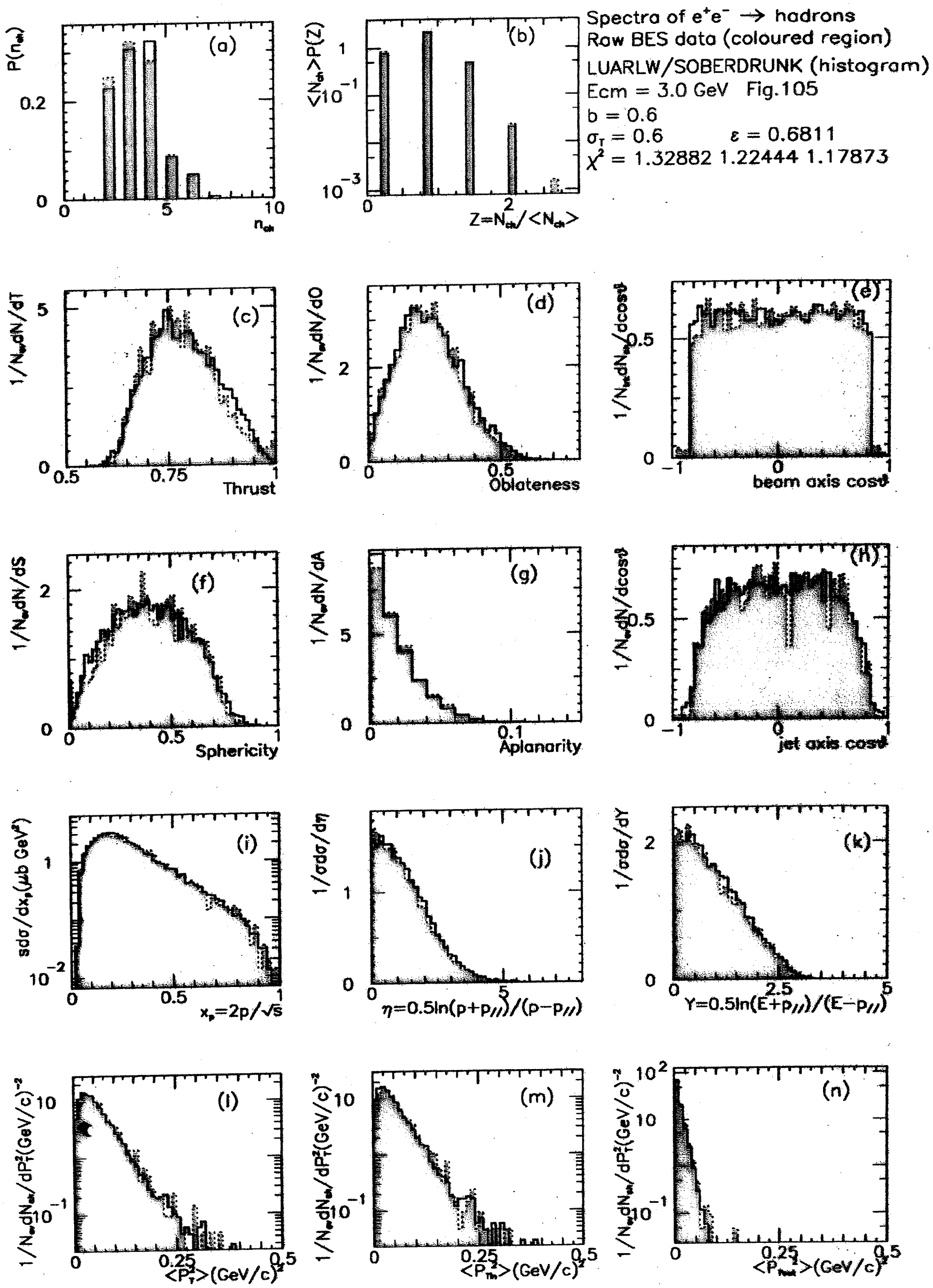

Figure 11: *$e^+e^- \rightarrow$ hadrons spectrum of raw BES data (grey region) and LUARLW/SOBDRUNK (black line) at $Ecm = 3.0$ GeV.*

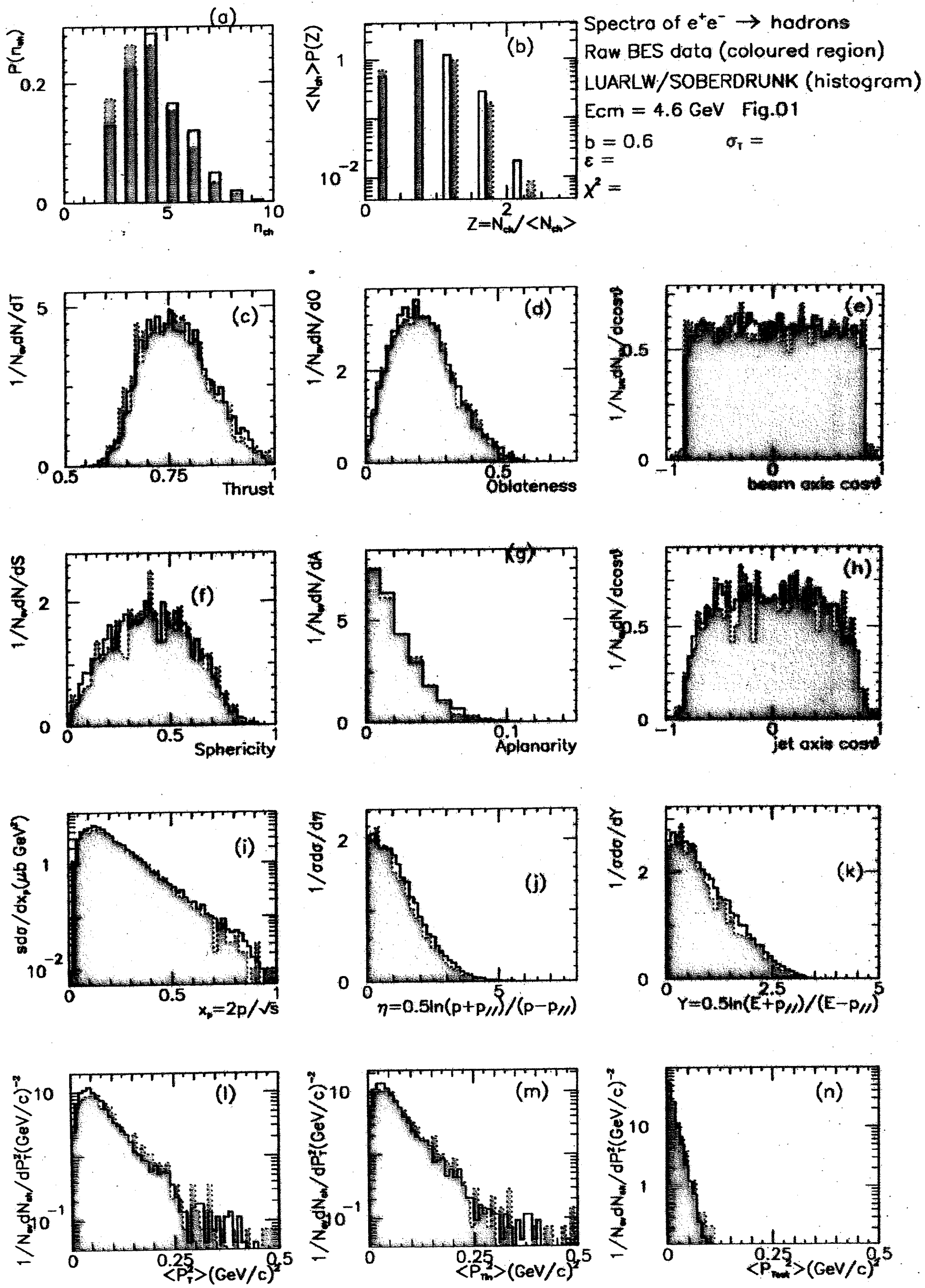

Figure 13: *$e^+e^- \rightarrow$ hadrons spectrum of raw BES data (grey region) and LUARLW/SOBDRUNK (black line) at $Ecm = 4.6$ GeV.*

Summary

$$\textbf{Lund MC}\begin{cases}\textbf{JETSET} & \textbf{high energy}\\ \textbf{Area Law} & \textbf{intermediate energy}\end{cases}$$

We develop the formalism to use the basic Lund Model area law directly for Monte Carlo program LUARLW, which will be satisfied to treat two-body up to six-body states.

The LUARLW predicts more than 14 distributions totally agree with BES data well.